A243 683

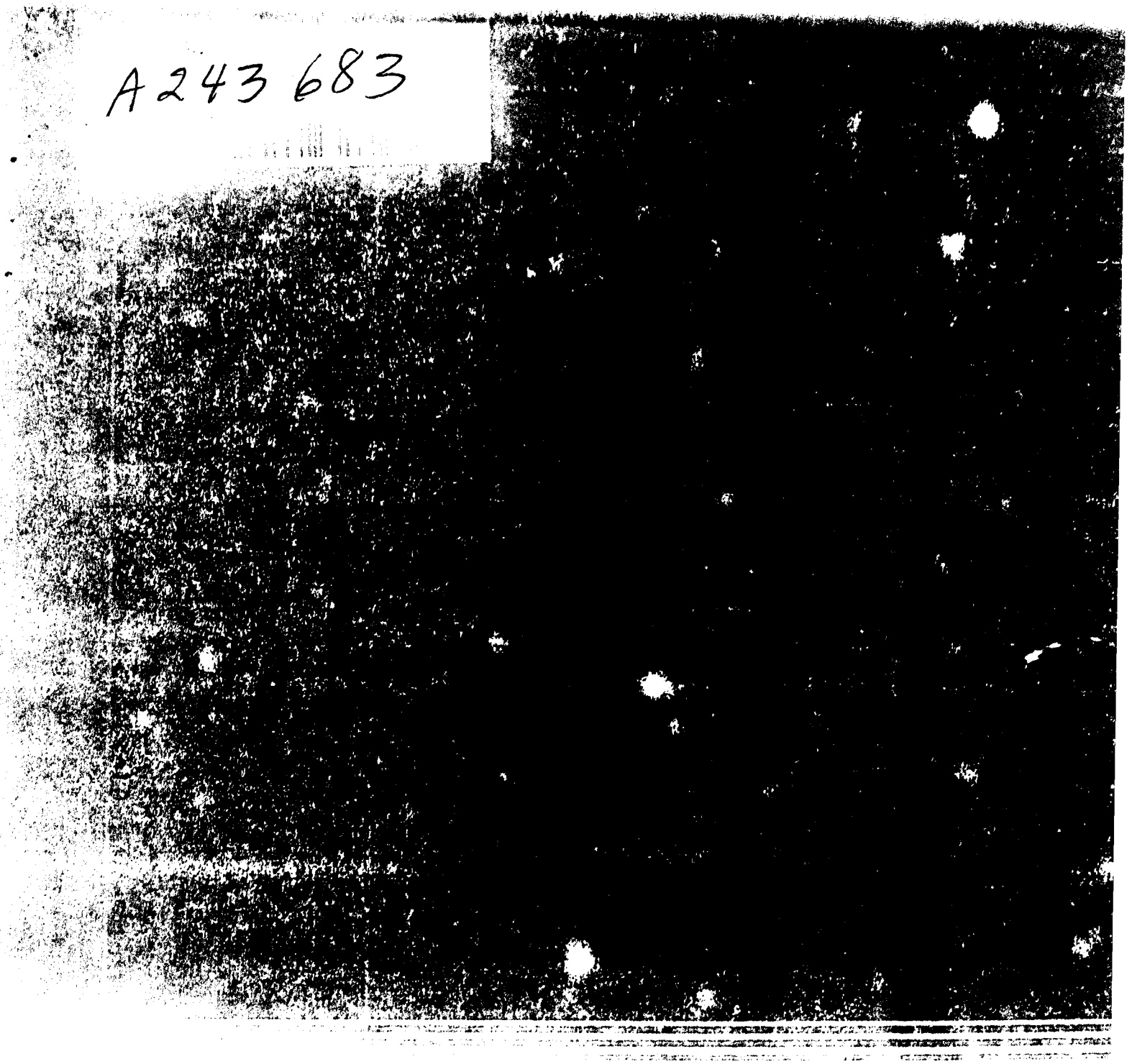

McDonnell Douglas Corporation

Magnetospheric Response to Variations in the Interplanetary Magnetic Field

Final Report

November 1991

N00014-89-C-0122

Final Report
submitted to the
Office of Naval Research

Prepared by: **K. A. Pfitzer**

Sr. Staff Manager - MDC Fellow

Approved by: **R. J. Reck**

Director
Design and Technology Center

Statement A per telecon Gracen Joiner
ONR/Code 1114
Arlington, VA 22217-5000

NWW 12/18/91

McDonnell Douglas Space Systems Company

ADVANCED PRODUCT DEVELOPMENT & TECHNOLOGY

5301 Bolsa Avenue, Huntington Beach, California 92647 (714) 896-3311

Table Of Contents

Section 1

INTRODUCTION AND BACKGROUND

It has been known for almost a quarter of a century that the extension of the geomagnetic field into space is limited by the flow of the solar wind past the vicinity of the earth. This theoretical prediction was confirmed early in the 1960's by direct satellite observation of both magnetopause and bow shock structures. Several major magnetospheric structures and processes have been discovered since that time. The extended antisolar region of the magnetosphere (the magnetospheric tail) was well documented by the mid-1960's. A cross section of the tail is characterized by a plasma sheet region through the center of the tail (on either side of the magnetic equator). The plasma sheet region separates the northern and southern lobe regions of the tail which are characterized by the relative lack of plasma and bundles of field lines directed toward (in the northern hemisphere) or away (in the southern hemisphere) from the earth. A current system flows through the plasma sheet region and returns at the magnetopause or just beyond it. These crosstail currents are responsible for the lobe structure of the magnetic field and the extended tail topology. In the early 1970's the high latitude magnetosphere was probed with satellites and it was found that there are two cusp regions where the shocked solar wind can penetrate directly to low altitudes. It is believed that a portion of the solar wind plasma directly enters the magnetosphere in these regions. In the mid-1970's further observations of the distant magnetosphere in the magnetopause region showed that a layer of the magnetosheath-like plasma persists just inside of the magnetopause. This boundary layer occurs just inside the magnetopause at almost all locations. The most recently discovered large scale structure in the magnetosphere is the field aligned current system inferred from its magnetic signatures.

All of these magnetospheric features persist at all times. This is not to say that they are steady. Rather, several of them exhibit a wide range of variability. For example, boundary layer thickness at a given location can vary from less than 100 kilometers to over 2000 kilometers. This variability is caused by the magnetosphere's response to changes in the solar wind and interplanetary magnetic field. Clearly, the magnetosphere's response to this variability is an important part in understanding the dynamics of the magnetospheric processes.

In both its ground state and as it responds to changes in solar wind and interplanetary magnetic field, the magnetosphere exerts a profound influence on the near earth orbital environment (the upper atmosphere and the ionosphere). In order to understand and predict this environment (and in some cases to mitigate against its effects) it is necessary to quantitatively understand the structures and processes which persist continuously in the magnetosphere. Studies by the National Academy of Sciences and the National Research Council in the early 1980's have listed the following as critical problems in understanding the magnetosphere:

- How does energy and plasma enter the magnetosphere?
- How is plasma transported within the magnetosphere?
- What are the sources of magnetic and electric fields in the magnetosphere (both their dc and ac components)?
- What are the mechanisms that link the magnetosphere to the earth's upper atmosphere and ionosphere?

Our magnetospheric work at MDAC over the past few years has centered on understanding physically the mechanisms for transfer of energy, mass, and momentum from the magnetosheath region into the magnetosphere, and on describing the interaction of the interplanetary magnetic field (IMF) with the magnetosphere. These are basic problems in magnetospheric physics since these processes must be understood before quantitative models of the many observed magnetospheric processes can be constructed. Such models are required for the prediction and specification of near earth orbital environmental "weather" parameters such as: trapped radiation fluxes, upper atmospheric density, ionospheric electron density, auroral particle precipitation and associated auroral luminosity, etc.

We have developed quantitative models of particle entry and solar wind and IMF influence on the magnetosphere. During this effort for ONR, our attention has been focused on the primary question: Is the substorm controlled by forces external to the magnetosphere or is it primarily a manifestation of processes occurring within the magnetospheric tail region?

Our models are driven by solar wind and IMF parameters. All parts of the models have been developed from first principles. It is our hope that in addition to shedding light on the substorm problem, the models will become useful in the truly predictive sense: that they can be used to anticipate the behavior of several of the routinely observed magnetospheric features and their subsequent effects on the upper atmosphere and ionosphere and the orbital systems that operate in that region.

The solar wind "entry" problem and the substorm have both been important problems in magnetospheric physics since the 1960s. Currently, both problems are explained primarily in terms of "reconnection theory", which we believe has major flaws. We discuss the entry problem first.

1.1 Solar Wind Entry into the Magnetosphere

The first magnetospheric problem to be considered theoretically was the calculation of the size and shape of the magnetosphere. They were determined by equating the solar wind pressure with the energy density (pressure) of the magnetospheric magnetic field. To make this three dimensional problem tractable, an assumption was made; that the solar wind particles were all specularly (mirror like) reflected off of the geomagnetic field, $\underline{B}$. This approximation to the real field was quite reasonable since the interaction region of the incident particles with $\underline{B}$ is very small (10s to 100s of km) compared to the scale size of the magnetospheric magnetic field (10s of thousands of km). This "pressure balance" formalism was used by many investigators to successfully determine the shape and size of the magnetosphere. The unfortunate legacy of this work, however, was the assumption that all of the solar wind particles are reflected off of the geomagnetic field and that none enters the magnetosphere.

Therefore, as early as 1960, concepts were already being suggested for the transfer of momentum across the boundary between interplanetary space (or more precisely, the magnetosheath) and the magnetosphere (the "viscous interaction" theories). Later, as the influence of the IMF on the magnetosphere became well established, the early work of Dungey and others on "reconnection" was suggested as another means for providing energy and mass to the magnetosphere from the solar wind. Several other concepts have been suggested: plasma instabilities along the magnetopause, a structured or "gusty" solar wind, and various diffusion processes.

The electron-electron collision frequency υ_{ee} is given by a similar analysis with a reduced mass $m_r = m_e/2$. Thus $\upsilon_{ee} = 2\ (10^{-6})\ sec^{-1}$. The total collision frequency for electrons, υ_e, is given by

$$\upsilon_e \approx \upsilon_{ei} + \upsilon_{ee} \approx 2.5 \times 10^{-6} / sec$$

The ion-ion collision frequency, υ_{ii}, is given by a similar formula, but since mr = $m_i/2 >> me$, υ_{ii} is negligible compared to υ_{ie}. Therefore the total collision frequency for ions, υ_i, is

$$\upsilon_i \approx \upsilon_{ie} \approx 2 \times 10^{-10} / sec$$

Since we are interested in disturbances with periods from minutes to weeks, the disturbance frequency ω ranges from 0.1 sec^{-1} to 10^{-6} sec^{-1}. We note that in our examination of the propagation of electromagnetic waves in the solar wind, the plasma parameters have the following properties:

$$\upsilon_i < \upsilon_e \lesssim \omega < \Omega_i < \Omega_e$$

The relations between these frequencies are important to the analysis that follows.

2.3.2 Propagation of Disturbances in Vacuum

It is instructive to first examine propagation in a vacuum. In a true vacuum, the ratio E to B is (E/Bc = 1). Therefore, in a vacuum, a 2 nT disturbance has associated with it an electric field of ~ 0.6 volts/meter. Thus it is obvious that we cannot use the vacuum approximation for magnetospheric work since the observed electric fields are smaller by at least three orders of magnitude.

We also note that the relativistic transformation for electromagnetic field are typically stated for vacuum conditions. Therefore, it is incorrect to assume that the presence of the interplanetary field as viewed from the earth reference frame produces in that frame (moving with velocity V with respect to the solar wind) an electric field. The question of interplanetary electric fields and their properties in the magnetosphere is in reality made much more complicated by the presence of plasma in the interplanetary region. Thus the dawn to dusk cross tail electric field that has been inferred to persist during periods of southward pointing interplanetary magnetic field is not only a gross oversimplification, but basically incorrect.

1.2 Problems with the Reconnection Theory

Another basic problem in magnetospheric physics is the understanding of the interaction of the IMF with the magnetosphere. Currently, most of the magnetospheric physics community chooses to represent this interaction in terms of reconnection theory. Basically, reconnection theory supposes that the two magnetic field sources (the IMF and $\underline{B}$) become "tied together" in the presence of a plasma. This process has the consequence of connecting the two magnetic fields such that field lines emanating from one are ultimately joined to the other source. An important by-product is the acceleration of charged particles in the "reconnection region". Proponents of reconnection theory suggest that it can explain the entry of the required solar wind plasma into the magnetosphere and also the relatively hot plasma observed in the tail of the magnetosphere.

We have several problems with this theory, however, and with support from ONR have developed an alternative physical description of the IMF and its interaction with the magnetosphere. Some of the problems we see in reconnection theory are as follows. Reconnection is dependent on the direction of the IMF which is observed to change, typically on the order of every few hours. Thus it is not clear to us how any reconnection process can drive any of the processes observed to persist at all times in the magnetosphere (e.g., the plasma sheet, the several magnetospheric currents, etc.). Its proponents state that reconnection takes place predominantly at the nose of the magnetopause and over the lobes of the tail. This poses the requirement of maintaining a complex electrostatic field at all times but in varying directions in order to permit particles entering there to journey to those regions where they are required (e.g., the plasma sheet). Finally, there is no conclusive evidence that this process operates in the IMF and magnetosphere even though a concerted effort has been expended searching for examples. A case in point was the AMPTE ion releases made upstream of the bow shock. No evidence was found for the presence of any ions entering near the nose of the magnetosphere even though the releases were performed during intervals of southward IMF (conditions favorable for dayside reconnection).

Section 2

TECHNICAL PRESENTATION

During the last few years we have worked on the entry of solar wind into the magnetosphere and on the control the interplanetary magnetic field (IMF) has on the magnetosphere. Correlative data conclusively prove that both the solar wind and the IMF exert considerable influence on magnetospheric processes, and the magnetospheric substorm in particular.

Our work on this subject may be roughly divided into two parts, particle entry and representation of the interaction of the IMF with the magnetosphere. We discuss particle entry first.

2.1 Particle entry

We have quantitatively determined where on the magnetopause that low energy (solar wind) charged particles can gain entry to the magnetosphere. To do this, we used a realistic quantitative model of the magnetospheric magnetic field. Particles of the same energy but differing incidence angles where then introduced to this field at a point on the magnetopause. It was found that at most points a finite "entry cone" persists. The entry cone is defined as that region (represented as a solid angle) through which particles have access to the magnetosphere. The value of the entry cone varies with particle energy and location on the magnetopause. We found that the entry cone was largest along the equatorial flanks of the tail. (An example of the entry cone is shown in Figure 1 and the size of the entry cone over the flanks of the tail is shown for protons in Figure 2.) The entry cone is exactly zero along the intersection of the noon-midnight meridian with the magnetopause by symmetry since there the particles really are specularly reflected.

Study of entry cone size suggests that no magnetosheath particles enter the magnetosphere over the lobes of the tail and also that no particles enter at the nose of the magnetosphere. The regions where entry does readily occur are along the sides (flanks) of the tail and in the vicinity of the dayside cusps. The "gradient drift" entry mechanism therefore supplies solar wind plasma directly to

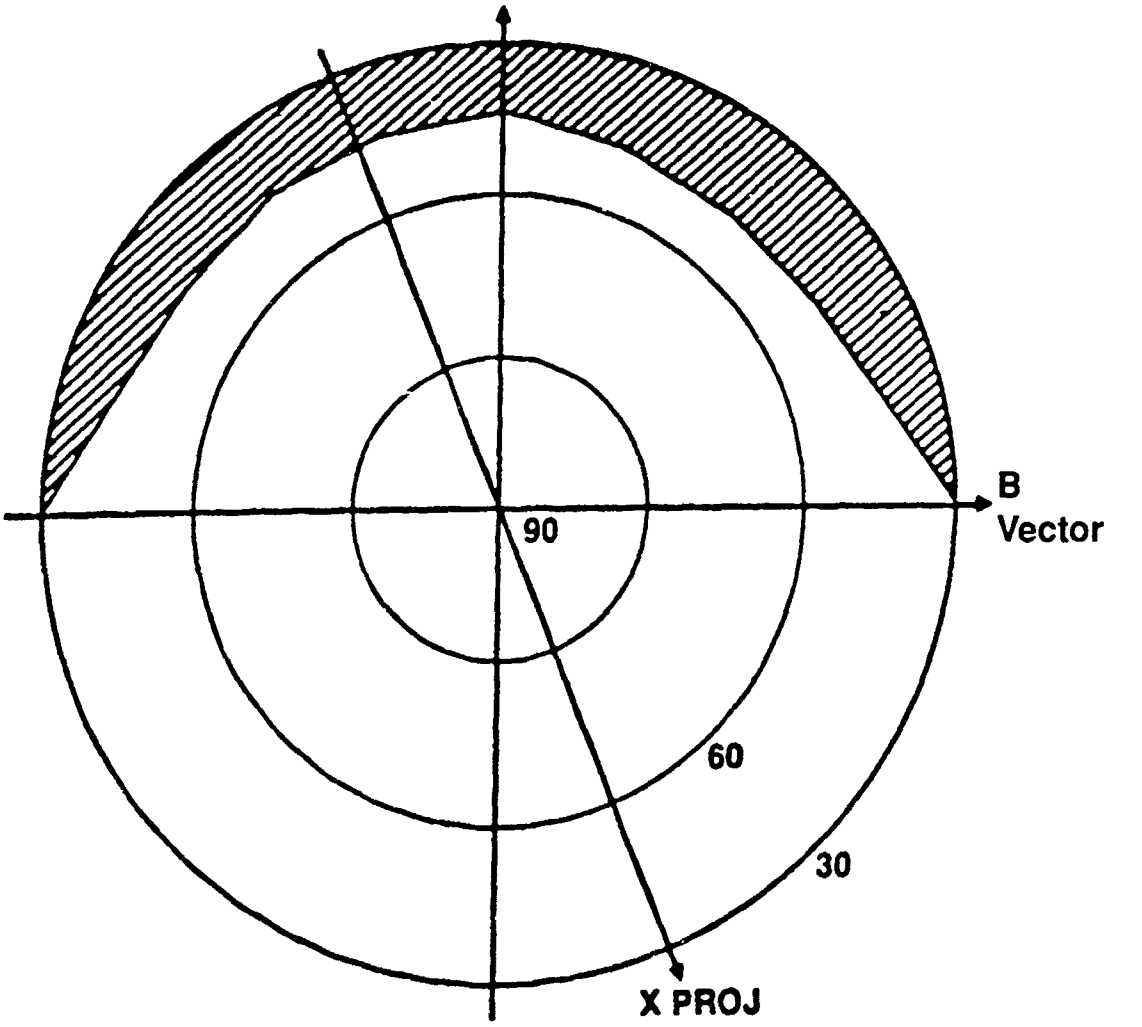

Figure 1. Description of an entry cone. The shaded portion represents the range of impact directions over which the particle gains entry to the magnetosphere. The boundary location is down the tail just above the magnetic equatorial plane (along the dawn flank). The projection of the x axis (in solar magnetospheric coordinates) and the direction of $\underline{B}$ at the entry point are shown. Particles moving away from the sun with a near grazing incidence are shown as "allowed" impact angles.

those regions of the magnetosphere where plasmas are observed (e.g., the plasma sheet in the tail and the dayside cusps). This is unlike the reconnection theories which introduce plasma near the nose of the magnetosphere and over the lobes of the tail. To date this work on particle entry has shown that particle entry depends on the strength of $\underline{B}$, its structure, and on the particle distribution function.

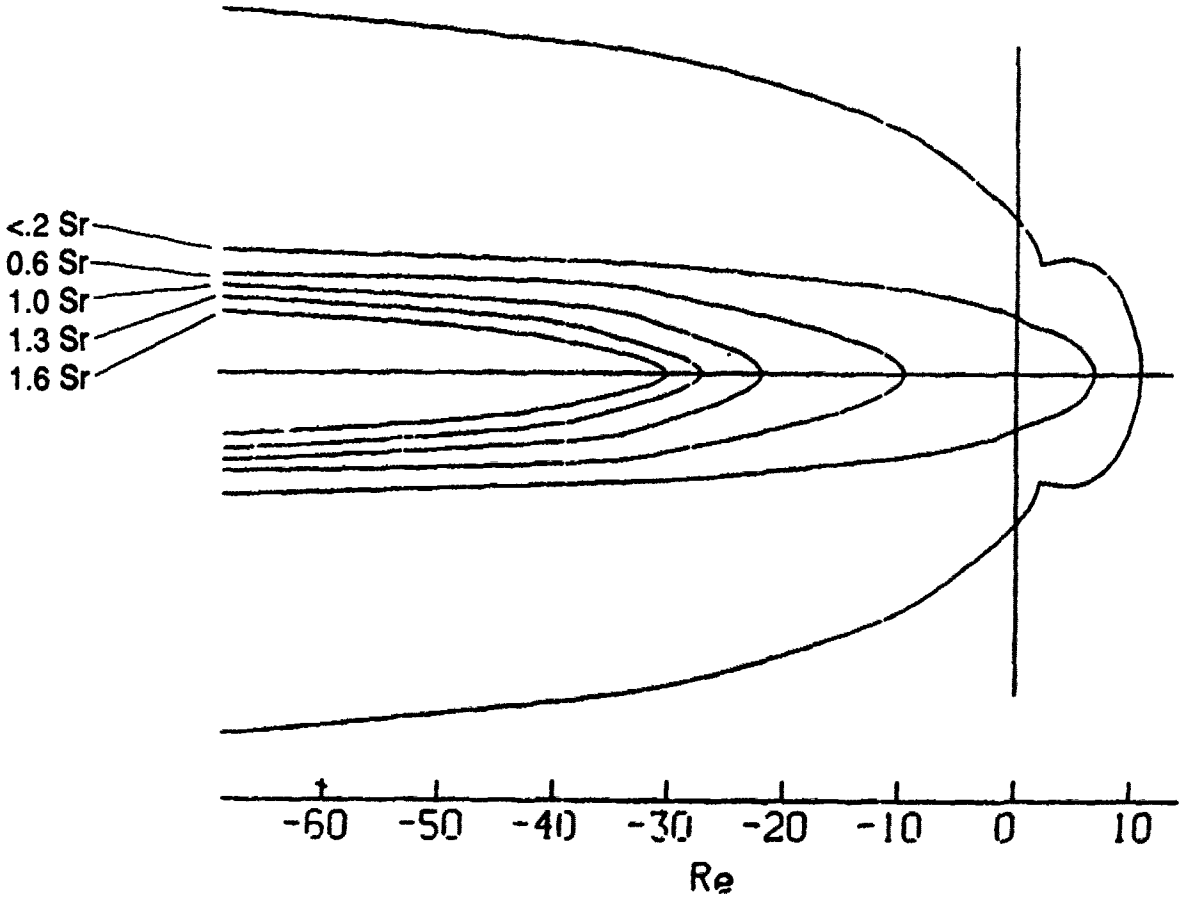

Figure 2. Contours of constant entry cone magnitude on the dawn side of the magnetosphere.

2.2 Representation of the Interplanetary Magnetic Field (IMF)

Correlative data establish beyond doubt that the IMF exerts considerable influence on magnetospheric processes. This subject has been exhaustively studied in terms of reconnection theory. We, however, have several complaints with reconnection theory (it introduces particles into the wrong regions of the magnetosphere: the IMF [and therefore the reconnection process] is continuously changing direction; there is little or no direct magnetospheric observational evidence for its existence etc.); and have, therefore, attempted to explain the interaction of the IMF with the magnetosphere in a way that we can understand the physics.

Basically, in this effort we have represented the IMF as the superposition of electromagnetic waves. The only limitation of our investigation is that we must

restrict it to wavelengths that are small with respect to the scale size of the magnetosphere. Thus we can examine only waves (or disturbances) with periods less than one hour. Although limited in this regard, our study sheds light on many aspects of the interaction of the IMF with the magnetosphere. We first present our findings on the propagation of electromagnetic disturbances in the solar wind. Interplanetary space is characterized by the continuous presence of both cnarged particles and a magnetic field. The most persistent feature of the interplanetary medium is the solar wind which flows approximately radially outward from the sun. The solar win is typically characterized in term of its bulk speed, thermal energy of both ions and electron, and its density. It is essentially electrically neutral. Its bulk speed has been observed to range from under 300 to over 1000 kilometers per second. The thermal energy of solar wind protons is approximately 10 eV corresponding to a thermal velocity of approximately 50 km/sec. The electron bulk speed is approximately the same as that of the protons, but the electron thermal velocity is approximately 2000 km/sec. The solar wind density is much more variable than its bulk speed, ranging from less that 0.1 to over 50 particle pairs per cubic centimeter.

The continuous flow of the solar wind is frequently interrupted by the passage of more energetic plasmas which also originate from the sun. There are many classes of interplanetary disturbances. All of them have shorter scale lengths and characteristic periods than the steady solar wind. We can therefore characterize the interplanetary plasma basically in terms of solar wind parameters if we understand that these average solar wind parameters are frequently perturbed by the passage of other plasmas.

Interplanetary space is also characterized by the presence of a magnetic field, commonly referred to as the interplanetary magnetic field (IMF). The strength of the IMF characteristically ranges from a large fraction of a nT to 25 nT. Typically its strength ranges from 2 to 25 nT. The interplanetary magnetic field, as will be shown below, is carried with the solar wind and is also perturbed by the passage of energetic plasmas. Like the interplanetary plasmas, the interplanetary magnetic field may be described as an average field (like the solar wind) perturbed by other fluctuating fields. The average field is produced by the 28 day rotation of the sun. It is referred to as the sector structure magnetic field and results on the average, in four distinct regions or sectors per 28 day rotation, in which the

magnetic field direction is primarily directed either toward or away from the sun. These sectors are referred to as toward and away sectors. This background portion of the magnetic field has a period of approximately 2 weeks and may, for all purposes, be considered a constant field when contrasted with the periodicity typically associated with the other magnetic disturbances which persist in the interplanetary space.

2.3 Propagation of Disturbances in the IMF - Basic analysis

In order to understand the interaction of the interplanetary magnetic field with the magnetosphere, we have first examined the propagation of electromagnetic disturbances in the interplanetary medium. Prior to the determination of allowed propagation modes, it is appropriate to examine some characteristic frequencies and other parameters in the interplanetary medium.

2.3.1 Characteristics of the IMF

The approximate plasma frequencies for solar wind electrons and protons are given by

$$(\omega_p)_j^2 = \frac{q_j^2 n_j}{m_j \varepsilon_o} \qquad (1)$$

where $(\omega_p)_j$ is the plasma frequency for the j^{th} species, n_j, q_j, and m_j are the number density, charge, and mass for the j^{th} species. The plasma frequency for protons $(w_p)_i$ and electron $(w_p)_e$ is then found to be in the range

$$\begin{aligned} (\omega_p) &\approx 4 \times 10^2 \text{ to } 10^4 \text{ / sec} \\ (\omega_e) &\approx 2 \times 10^4 \text{ to } 4 \times 10^5 \text{ / sec} \end{aligned} \qquad (2)$$

The cyclotron frequency is given by

$$\Omega_j = \frac{q_j B}{m_j} \qquad (3)$$

Thus if the magnetic field, B, is in the range 1 to 50 nT, the cyclotron frequencies are:

$$\Omega_i = 0.1 \text{ to } 5 \text{ / sec for protons}$$
$$\Omega_e = 200 \text{ to } 10^4 \text{ / sec for electrons} \qquad (4)$$

The Debye shielding length, λ_D, is given by

$$\lambda_D = k_D^{-1} \qquad (5)$$

where

$$k_D = \frac{(\omega_p)_e}{\sqrt{\bar{v}_e^2}} + \frac{(\omega_p)_i}{\sqrt{\bar{v}_i^2}}$$

$\bar{v}_e$ and $\bar{v}_i$ are the r.m.s. thermal speed of the electrons and protons. We note that the electron and ion species contribution to k_D are approximately equal. Thus typically in the solar wind the Debye length is

$$\lambda_D \approx 2.5 \text{ to } 50 \text{ meters}$$

Therefore, within a Debye sphere $n_p\lambda_D^3$ and $n_e\lambda_D^3 >> 1$. It is therefore appropriate to treat the solar wind as a plasma and to use the plasma collective mode equations to describe electromagnetic processes present there.

Also, since the highest frequency disturbance do not exceed 10^{-2} Hz, their wavelength far exceeds the Debye length λ_D and the long wavelength approximation can be used.

Another plasma parameter of importance in this analysis is the collision frequency. The dominant collision mechanism is the close-in collision between the charged particles due to the coulomb force. This coulomb scattering (Rutherford) is described in many texts (for example, see Jackson, 1962 and Davies, 1966)

The momentum transfer collision frequency of the electrons due to the interactions with the protons (ions), υ_{ei}, is

$$\upsilon_{ei} = n_i \sigma_R \bar{V} \left(\overline{1 - \cos\theta}\right) \qquad (6)$$

where n_i is the ion density, σ_R is the Rutherford cross section, $\overline{V}$ is the average speed between particles (approximately the r.m.s. electron thermal speed of 2 x 10^6 m/sec) and $\left(\overline{1-\cos\theta}\right)$ is the mean change in the direction cosine of the electrons caused by the proton. Rutherford scattering theory gives

$$\left(\overline{1-\cos\theta}\right) \approx \frac{\overline{\theta^2}}{2} = \theta_{min}^2 \, \ell n \left(\frac{\theta_{max}}{\theta_{min}}\right) \tag{7}$$

where θ_{min} is the minimum scattering angle and θ_{max} is the maximum scattering angle. The ratio

$$\frac{\theta_{max}}{\theta_{min}} = \frac{12\pi n_i}{k_D^3} \tag{8}$$

For a screened plasma of temperature $k_B T \leq$ Rydberg (13.7 eV), where k_B is the Boltzman constant and T is the temperature. The Rutherford cross section is

$$\sigma_r = \left|\frac{2 Z_e Z_i e^2}{p \tilde{v}}\right| \frac{2\pi}{\theta_{min}^2} \tag{9}$$

where

$Z_e = Z_i = 1$ the charge of the two species

$p = M_r v$, and

$1/M_r = 1/m_r + 1/m_e$, the reduced mass cross $M_r = m_e$ because m_i is much greater than m_e; therefore, by combining equations 6-9, one has

$$\upsilon_{ei} = \frac{4 \pi n_i e^4}{M_r^2 \tilde{v}^3} \ell n \left(\frac{12 \pi n_i}{k_D^3}\right) \tag{10}$$

Since $k_D = 2(\omega_p)_e / \tilde{v}$ and for the case of $n_i = 5$/cc (Note: Eq. 10 is in unrationalized c.g.s. units), one gets $\upsilon_{ei} = 5 \times 10^{-7}$ /sec.

The momentum transfer collision for ions due to collision with electrons is a factor $m_e/M_i = 1/2000$ smaller than v_{ei}, therefore $\upsilon_{ie} = 2(10^{-10})$ sec^{-1} for the above specified plasma density.

The electron-electron collision frequency υ_{ee} is given by a similar analysis with a reduced mass $m_r = m_e/2$. Thus $\upsilon_{ee} = 2\ (10^{-6})\ sec^{-1}$. The total collision frequency for electrons, υ_e, is given by

$$\upsilon_e \approx \upsilon_{ei} + \upsilon_{ee} \approx 2.5 \times 10^{-6} / sec$$

The ion-ion collision frequency, υ_{ii}, is given by a similar formula, but since mr = $m_i/2 >> me$, υ_{ii} is negligible compared to υ_{ie}. Therefore the total collision frequency for ions, υ_i, is

$$\upsilon_i \approx \upsilon_{ie} \approx 2 \times 10^{-10} / sec$$

Since we are interested in disturbances with periods from minutes to weeks, the disturbance frequency ω ranges from 0.1 sec^{-1} to 10^{-6} sec^{-1}. We note that in our examination of the propagation of electromagnetic waves in the solar wind, the plasma parameters have the following properties:

$$\upsilon_i < \upsilon_e \lesssim \omega < \Omega_i < \Omega_e$$

The relations between these frequencies are important to the analysis that follows.

2.3.2 Propagation of Disturbances in Vacuum

It is instructive to first examine propagation in a vacuum. In a true vacuum, the ratio E to B is (E/Bc = 1). Therefore, in a vacuum, a 2 nT disturbance has associated with it an electric field of ~ 0.6 volts/meter. Thus it is obvious that we cannot use the vacuum approximation for magnetospheric work since the observed electric fields are smaller by at least three orders of magnitude.

We also note that the relativistic transformation for electromagnetic field are typically stated for vacuum conditions. Therefore, it is incorrect to assume that the presence of the interplanetary field as viewed from the earth reference frame produces in that frame (moving with velocity V with respect to the solar wind) an electric field. The question of interplanetary electric fields and their properties in the magnetosphere is in reality made much more complicated by the presence of plasma in the interplanetary region. Thus the dawn to dusk cross tail electric field that has been inferred to persist during periods of southward pointing interplanetary magnetic field is not only a gross oversimplification, but basically incorrect.

2.3.3 Propagation of Disturbances in the Presence of a Plasma

2.3.3.1 General Equations

To treat the general case of electromagnetic waves in the solar wind, it is first noted that the frequency range of disturbances observed in the IMF is many orders of magnitude lower than the frequency of wave phenomena typically studied in the laboratory. Yet, we will find that magnetic disturbances present in the solar wind are not magnetostatic but electromagnetic waves. To represent electromagnetic waves in the presence of a plasma, it is customary to begin with Maxwell's equations.

If the plasma has disturbances at the angular frequency, ω (sec^{-1}), then the electric field, $\underline{E}$, and the magnetic field, $\underline{B}$, can be written

$$\underline{E} = \underline{E}_o e^{i\omega t}$$
$$\underline{B} = \underline{B}_o e^{i\omega t} \qquad (11)$$

where $\underline{B}_o$ and $\underline{E}_o$ are dependent only on position and t the time.

Maxwell's equations in rationalized MKS units in frequency space can be written

$$\nabla \times \underline{E} = -i\omega \underline{B}$$
$$\nabla \times \underline{B} = \mu_o \underline{J} + \frac{i\omega}{c^2}\underline{E}$$
$$\nabla \cdot \underline{B} = 0 \qquad (12)$$
$$\nabla \underline{E} = \frac{\rho}{\varepsilon_o}$$

where

$$\mu_o = 4\pi(10^{-7}) \text{henries/m}$$
$$\varepsilon_o = 8.85(10^{-12}) \text{farad/m}$$
$$c = 3(10^8) \text{m/s}$$

and ρ and $\underline{J}$ are the total charge and current densities respectively.

It is convenient to break the charge and current sources (ρ and $\underline{J}$) into externally driven sources (ρ_{ext} and $\underline{J}_{ext}$) and sources produced locally (ρ_{ind} and $\underline{J}_{ind}$) by polarization effects.

Thus

$$\begin{aligned}\rho &= \rho_{ext} + \rho_{ind} = \rho_{ext} - \nabla\cdot(\varepsilon_\circ \underline{\underline{X}}\cdot\underline{E}) \\ \underline{J} &= \underline{J}_{ext} + \underline{J}_{ind} = \underline{J}_{ext} + \underline{\underline{\sigma}}\cdot\underline{E}\end{aligned} \tag{13}$$

where $\underline{\underline{X}}$ and $\underline{\underline{\sigma}}$ are the tensor functions for susceptibility and conductivity.

The curl of equation (12) yields

$$\begin{aligned}\nabla x \nabla x \underline{E} &= -i\omega \nabla x \underline{B} \\ \nabla(\nabla\cdot\underline{E}) - \nabla\cdot\nabla\underline{E} &= -i\omega\nabla x \underline{B}\end{aligned} \tag{14}$$

Since

$$\nabla x \underline{B} = \mu_\circ \underline{J} + \frac{i\omega}{c^2}\underline{E}$$

$$\nabla\cdot\underline{E} = \frac{\rho}{\varepsilon_\circ}$$

it follows that

$$\nabla\left(\frac{\rho}{\varepsilon_\circ}\right) - \nabla^2\underline{E} = -i\omega\left(\mu_\circ \underline{J} + \frac{\omega}{c^2}\underline{E}\right) \tag{15}$$

Substituting for ρ and $\underline{J}$ by using equation (13)

$$-\nabla^2\underline{E} - \frac{\omega^2}{c^2}\underline{E} - \nabla(\nabla\cdot\underline{\underline{X}}\cdot\underline{E}) + i\mu_\circ\omega\underline{\underline{\sigma}}\cdot\underline{E} = -i\omega\mu_\circ\underline{J}_{ext} - \nabla\left(\frac{\rho_{ext}}{\varepsilon_\circ}\right) \tag{16}$$

Note that equation 16 is in the frequency space-domain, and

$$\underline{E} = \underline{E}(\omega, \underline{r}) = \underline{E}(\underline{r})\, e^{i\omega t}$$

The Fourier transform of the space domain into wave numbers, $\underline{k}$, permits the substitution of a differential equation (16) by an algebraic equation (replacing ∇ with $i\underline{k}$). Thus

$$(k^2 - \frac{\omega^2}{c^2})\underline{E} + \underline{k}(\underline{k}\cdot\underline{\underline{X}}\cdot\underline{E}) + i\mu_o\omega\underline{\underline{\sigma}}\cdot\underline{E} = -i(k\frac{\rho_{ext}}{\varepsilon_o} + \mu_o\omega\underline{J}_{ext}) \qquad (17)$$

The right side of equation (17) represents the transform of the various source terms creating the disturbance. When these source terms are known, the algebraic equation can be solved. Then, by inverting the transform, the space time dependence of the fields is obtained.

we seek field patterns that can exist (i.e., frequency and wave number relations) without being continually excited (i.e., that can propagate in the solar wind plasma). They are obtained by setting the right side of equation (17) to zero. For a non-zero solution of the resulting homogeneous equation, the determinant of the coefficients must vanish such that

$$\det\left\{\left(k^2 - \frac{\omega^2}{c^2}\right)\underline{\underline{I}} + \underline{k}(\underline{k}\cdot\underline{\underline{X}}) + i\mu_o\omega\underline{\underline{\sigma}}\right\} = 0 \qquad (18)$$

To solve equation (18), it is necessary to develop a relationship between the tensor electrical conductivity, $\underline{\underline{\sigma}}$, and the magnetic susceptibility, $\underline{\underline{X}}$. Since the solar wind is known to be almost perfectly charge neutral at all times, conservation of charge can be used to provide the required relationship. Thus

$$\nabla\cdot\underline{J}_{ext} + \frac{\partial\rho_{ext}}{\partial t} = 0 \qquad (19)$$

then by substituting for $\underline{J}_{ind}$ and ρ_{ind}, we get

$$\nabla\cdot(\underline{\underline{\sigma}} - i\omega\varepsilon_o\underline{\underline{X}})\cdot\underline{E} = 0 \qquad (20)$$

As mentioned earlier, for the frequencies of interest (of magnetic disturbances in the solar wind) the long wavelength approximation can be used. Thus

$$\underline{\underline{\sigma}} = i\omega\varepsilon_o\underline{\underline{X}} \qquad (21)$$

Using equation (21), equation (18) can be written in terms of only $\underline{\underline{X}}$.

$$\det\left\{\left(k^2-\frac{\omega^2}{c^2}\right)\underline{\underline{I}}+\underline{k}(\underline{k}\cdot\underline{X})-\frac{\omega^2}{c^2}\underline{\underline{X}}\right\}=0 \tag{22}$$

To arrive at the solution to equation (22) and provide the appropriate relation between k and w, we must first arrive at a solution to the susceptibility tensor $\underline{\underline{X}}$.

The cold plasma and long wavelength characteristics are most easily obtained from Lorentz force equation with collisional damping (used by Appleton in his ionospheric work of the 1930's)

$$m_j\frac{d\underline{V}_j}{dt}=q_j\left(\underline{E}+\underline{V}_j\times\underline{B}_{amb}\right)-\upsilon_j m_j\underline{V}_j \tag{23}$$

where

m_j is the mass of the j^{th} particle

V_j is the frequency transform of the velocity vector of the j^{th} particle species

q_j is the charge

v_j is the collisional frequency damping of the jth particle species

$\underline{B}_{amb}$ is the ambient magnetic field

In this work only two particle species are important, protons and electrons. If we let the subscript j = e for electrons and j = i for protons (ions), then

$m_e = 9.1\ (10^{-31})$ kg

$m_i = 1.6\ (10^{-27})$ kg

$q_e = +e = 1.6 \times 10^{-19}$ coulomb

$q_i = -e = -1.6 \times 10^{-19}$ coulomb

Furthermore, since $(\underline{V}_j \cdot \nabla \underline{V}_j)\,\underline{V}_j << \partial V_j / \partial t$ in the long wavelength approximation, then

$$\frac{d\underline{V}_j}{dt} = \frac{\partial \underline{V}_j}{\partial t}$$

Equation (23) can be rewritten as

$$i\omega \underline{V}_j = \frac{q_j}{m_j}\left(\underline{E} + \underline{V}_j \times \underline{B}_{amb}\right) - \upsilon_j \underline{V}_j \tag{24}$$

This above vector equation is a set of coupled linear equations and can be solved for $\underline{V}_j$ in a straight forward manner. To solve this set of equations, a right handed coordinate system is defined with unit vectors $\underline{\alpha}$, $\underline{\beta}$, $\underline{\gamma}$, where $\underline{\gamma}$ is the direction of the ambient magnetic field, $\underline{B}_{amb}$ and $\underline{\gamma} = \underline{\alpha} \times \underline{\beta}$. To simplify the algebra, we define the cyclotron frequency of the j^{th} species, Ω_j, as $\Omega_j = q_j \underline{B}_{amb}/m_j$. Solving equation (24) one gets

$$\begin{aligned}
(V_j)_\alpha &= -\frac{i\frac{q_j}{m_j}(\omega - i\upsilon_j)}{(\omega - i\upsilon_j)^2 - \Omega_j^2} E_\alpha - \frac{\frac{q_j}{m_j}\Omega_j}{(\omega - i\upsilon_j)^2 - \Omega_j^2} E_\beta \\
(V_j)_\beta &= -\frac{i\frac{q_j}{m_j}(\omega - i\upsilon_j)}{(\omega - i\upsilon_j)^2 - \Omega_j^2} E_\beta + \frac{\frac{q_j}{m_j}\Omega_j}{(\omega - i\upsilon_j)^2 - \Omega_j^2} E_\alpha \\
(V_j)_\gamma &= -\frac{i\frac{q_j}{m_j}}{(\omega - i\upsilon_\gamma)} E_\gamma
\end{aligned} \tag{25}$$

Since

$$(\underline{J}_{nd})_j = \underline{\sigma}_j \cdot \underline{E} \tag{27}$$

where n_j is the density of the J^{th} species then

$$q_j n_j V_j = \underline{\sigma}_j \cdot \underline{E} \tag{28}$$

substituting into equation (21) gives

$$\frac{q_j n_j}{i\omega\varepsilon_\circ}\underline{V}_j = \underline{\underline{X}}_j \cdot \underline{E} \tag{29}$$

Thus one can write the complex susceptibility tensor as

$$\begin{aligned}
(X_j)_{\alpha\alpha} &= (X_j)_{\beta\beta} = \frac{-(\omega_p)_j^2(\omega - i\upsilon_j)}{\omega\left[(\omega - i\upsilon_j)^2 - \Omega_j^2\right]} \\
(X_j)_{\gamma\gamma} &= \frac{-(\omega_p)_j^2}{\omega(\omega - i\upsilon_j)} \\
(X_j)_{\alpha\beta} &= (X_j)_{\beta\alpha} = \frac{i(\omega_p)_j^2\Omega_j}{\omega\left[(\omega - i\upsilon_j)^2 - \Omega_j^2\right]}
\end{aligned} \tag{30}$$

$$(X_j)_{\alpha\gamma} = (X_j)_{\gamma\alpha} = (X_j)_{\beta\gamma} = (X_j)_{\gamma\beta} = 0$$

where

$$(\omega_p)_j^2 = \frac{q_j^2 n_j}{m_j \varepsilon_\circ} \quad \text{and} \quad \Omega_j = q_j \frac{B}{m_j}$$

$(\omega_p)_j$ is the plasma frequency and Wj is the cyclotron frequency for the j^{th} species.

The values of the susceptibility tensor are now substituted into equation (22) and expanding this equation into component form one gets

$$\begin{vmatrix} A + k_\alpha m & C + k_\alpha n & k_\alpha q \\ -C + k_\beta m & A + k_\beta n & k_\beta q \\ k_\gamma m & k_\gamma n & B + k_\gamma q \end{vmatrix} = 0$$

where

$$A = k^2 - \frac{\omega^2}{c^2}(1 + X_{\alpha\alpha})$$
$$B = k^2 - \frac{\omega^2}{c^2}(1 + X_{\gamma\gamma}) \qquad (31)$$
$$C = -\frac{\omega^2}{c^2} X_{\alpha\beta}$$

$$m = (k \cdot X)_\alpha = k_\alpha X_{\alpha\alpha} + k_\beta X_{\beta\alpha} = k_\alpha X_{\alpha\alpha} - k_\beta X_{\alpha\beta}$$
$$n = (k \cdot X)_\beta = k_\alpha X_{\alpha\beta} + k_\beta X_{\beta\beta} = k_\alpha X_{\alpha\beta} + k_\beta X_{\alpha\alpha}$$
$$q = (k \cdot X)_\gamma = k_\gamma X_{\gamma\gamma}$$

(m, n, q are the projections of the $\underline{\underline{X}}$ tensor on the $\underline{k}$ vector and k_α, k_β, and k_γ are the components of the $\underline{k}$ vector in the $\underline{\alpha}$, $\underline{\beta}$, and $\underline{\gamma}$ directions.)

Expanding the determinant gives

$$A^2B + AB(k_\alpha m + k_\beta n) + A^2 k_\gamma q + BC^2 + BC(k_\alpha n - k_b m) + C^2 k_\gamma q = 0 \qquad (32)$$

If we define the transverse component of the $\underline{k}$ vector, k_T, as $k_T = k_\alpha \alpha + k_\beta \beta$, thus

$$k_T^2 = k_\alpha^2 + k_\beta^2 \qquad (33)$$

then

$$k_\alpha m + k_\beta n = k_T^2 X_{\alpha\alpha}$$
$$k_\alpha n - k_\beta m = k_T^2 X_{\alpha\beta} \qquad (34)$$
$$k_\gamma q = k_\gamma^2 X_{\gamma\gamma}$$

where

$$\left\{\left[k^2-\frac{\omega^2}{c^2}(1+X_{\alpha\alpha})\right]^2+\left[\frac{\omega^2}{c^2}X_{\alpha\beta}\right]^2\right\}\left\{k^2-\frac{\omega^2}{c^2}(1+X_{\gamma\gamma})+k_\gamma^2X_{\gamma\gamma}\right\}$$

$$+k_T^2\left[k^2-\frac{\omega^2}{c^2}(1+X_{\gamma\gamma})\right]\left[\left(k^2-\frac{\omega^2}{c^2}\right)X_{\alpha\alpha}-\frac{\omega^2}{c^2}\left(X_{\alpha\alpha}^2-X_{\alpha\beta}^2\right)\right]=0 \qquad (35)$$

2.3.3.2 Propagation in a Plasma with No Background Magnetic Field

We now apply the above set of equations to the magnetospheric disturbance problems. We first examine the propagation of a disturbance (a wave of frequency ω) through the solar wind when no steady magnetic field is present. When B = 0, the cyclotron frequencies for both electrons and ions are zero. Setting Ω_i and Ω_e to zero and solving equation (35) gives

$$X_{\alpha\beta}=X_{\beta\alpha}=0$$
$$(X_j)_{\alpha\alpha}=(X_j)_{\beta\beta}=(X_j)_{\gamma\gamma} \qquad (36)$$

if we let

$$X=(X_i)_{\alpha\alpha}+(X_e)_{\alpha\alpha}=(X_i)_{\beta\beta}+(X_e)_{\beta\beta}=\ldots..$$

then

$$X=-\frac{(\omega_p)_i^2}{\omega(\omega-i\upsilon_i)}-\frac{(\omega_p)_e^2}{\omega(\omega-i\upsilon_e)} \qquad (37)$$

If we take equation (35) and apply the condition in (36), we get

$$\left[k^2-\frac{\omega^2}{c^2}(1+X)\right]^2\left[k^2-\frac{\omega^2}{c^2}(1+X)+k_\gamma^2X\right]$$
$$+k_T\left[k^2-\frac{\omega^2}{c^2}(1+X)\right]^2\left[\left(k^2-\frac{\omega^2}{c^2}\right)X-\frac{\omega^2}{c^2}X^2\right]=0 \qquad (38)$$

This equation can be satisfied if

$$k^2 - \frac{\omega^2}{c^2}(1+X) = 0 \tag{39}$$

We can substitute equation (37) into (38) and since $\omega_p >> \omega$ and $|X| >> 1$, one gets

$$k^2 = \frac{\omega^2}{c^2}\left[1 - \frac{(\omega_p)_i^2}{\omega(\omega - i\upsilon_i)} - \frac{(\omega_p)_e^2}{\omega(\omega - i\upsilon_e)}\right] \tag{40}$$

Furthermore, since $(\omega_p)_e >> (\omega_p)_i$, we can drop the first term and thus write

$$k^2 \approx \frac{-(\omega_p)_e^2}{c^2}\frac{\omega^2}{(\omega^2 + \upsilon_e^2)} - i\frac{(\omega_p)_e^2}{c^2}\frac{\omega\upsilon_e}{(\omega^2 + \upsilon_e^2)} \tag{41}$$

Since the real part of the above equation is always negative, there is no solution for k. Furthermore, since ω is on the same order or larger than υ_e, the magnitude of the complex k is approximately $(\omega_p)_e/c$, which is on the order of 10^{-4} to 10^{-3} /meter. Over length of 1 to 10 km, any electromagnetic wave will be Debye shielded. Thus we find that the electromagnetic waves cannot propagate in the solar wind plasma when it does not possess a steady background magnetic field unless they are continuously driven by local sources. In other words, any electromagnetic disturbance formed in the solar wind source will die out over a scale length of 1 to 10 km if no background magnetic field is present.

2.3.3.3 Propagation in a Plasma With an Imbedded Magnetic Field

Magnetic disturbances can be classified into roughly two categories; high frequency perturbations and the very low frequency disturbances associated with the 28 day sector structure magnetic rotation of the sun. The frequency associated with the 28 day period magnetic field is so much lower than the range of disturbance frequencies of interest that is may be considered for our purposes to provide a background magnetic field to the solar wind.

Generally, in the presence of both plasma and an imbedded steady state magnetic field, the ratio of $E/Bc = \omega/kc = \omega/\omega_p$. Since $\omega << \omega_p$, the electric field

associated with magnetic variations in the solar wind is very small. For the 28 day solar rotation source, the resultant electric field of approximately 10^{-9} volt/meter is much smaller than observed. Thus the observed interplanetary electric field (10^{-6} to 10^{-4} Volt/meter) must be produced by the higher frequency disturbances (on the order of hours or minutes) in which we are interested.

We now show that these higher frequency disturbances are allowed to propagate in the solar wind when it contains a background magnetic field associated with the sun's rotation (the solar sector magnetic field).

We have shown quite generally that for a low frequency wave to propagate without excessive damping and with the proper E/B relationship, the presence of a plasma and a background steady magnetic field are both required.

To examine the propagation of electromagnetic disturbances in the solar wind (containing "ambient" solar sector magnetic field), it is convenient to examine two distinct cases: 1) propagation along ambient magnetic field, and 2) propagation normal to the ambient magnetic field.

2.3.3.3.1 Propagation Parallel to B

For propagation along the ambient field

$$k_T = 0$$

$$k^2 = k_\gamma^2$$

Thus the dispersion relation, Equation (35) can be written as

$$\left\{\left[k_\gamma^2 - \frac{\omega^2}{c^2}(1+X_{\alpha\alpha})\right]^2 + \left(\frac{\omega^2}{c^2}X_{\alpha\beta}\right)^2\right\}(1+X_{\gamma\gamma})\left(k_\gamma^2 - \frac{\omega^2}{c^2}\right) = 0 \qquad (42)$$

Here, the first factor is zero if

$$k_\gamma^2 = \frac{\omega^2}{c^2}(1+X_{\alpha\alpha} \pm iX_{\alpha\beta})$$

Using the values for X_i and X_e, and substituting for $X_{\alpha\alpha}$ and $X_{\alpha\beta}$ yields

$$X_{\alpha\alpha} \pm iX_{\alpha\beta} = -\frac{(\omega_p)_i^2(\omega - i\upsilon_i)}{\omega\left[(\omega - i\upsilon_i)^2 - \Omega_i^2\right]} - \frac{(\omega_p)_e^2(\omega - i\upsilon_e)}{\omega\left[(\omega - i\upsilon_e)^2 - \Omega_e^2\right]}$$
$$\pm \frac{i\cdot i(\omega_p)_i^2\Omega_i}{\omega\left[(\omega - i\upsilon_i)^2 - \Omega_i^2\right]} \pm \frac{i\cdot i(\omega_p)_e^2\Omega_e}{\omega\left[(\omega - i\upsilon_e)^2 - \Omega_e^2\right]} \qquad (43)$$

Simplifying gives

$$X_{\alpha\alpha} \pm iX_{\alpha\beta} = -\frac{-(\omega_p)_i^2}{\omega(\omega - in_i + \Omega_i)} - \frac{-(\omega_p)_e^2}{\omega(\omega - in_e + \Omega_e)}$$
$$= \frac{-(\omega_p)_i^2}{\mp\Omega_i\omega\left(1 \mp \frac{\omega - i\upsilon_i}{\Omega_i}\right)} - \frac{-(\omega_p)_e^2}{\mp\Omega_e\omega\left(1 \mp \frac{\omega - i\upsilon_e}{\Omega_e}\right)} \qquad (44)$$

Since υ_i and $\omega << \Omega_i$, and υ_e and $\omega << \Omega_e$

and since $\frac{1}{1 \pm \xi} = 1 \mp \xi + 0(\xi^2)$ for $\xi << 1$

and since $\frac{(\omega_p)_i^2}{\Omega_i} = \frac{-(\omega_p)_e^2}{\Omega_e}$ when $n_e = n_i$

then

$$X_{\alpha\alpha} \pm iX_{\alpha\beta} \approx \frac{(\omega_p)_i^2}{\Omega_i^2}\left(\frac{\omega - i\upsilon_i}{\omega}\right) + \frac{(\omega_p)_i^2}{\Omega_i\,\Omega_e}\left(\frac{\omega - i\upsilon_e}{\omega}\right) \qquad (45)$$

utilizing the facts

$$\Omega_e = \frac{m_i}{m_e}\Omega_i$$

$$\frac{m_i}{m_e} >> 1$$

one gets

$$X_{\alpha\alpha} \pm i X_{\alpha\beta} \approx \frac{(\omega_p)_i^2}{\Omega_i^2}\left[\frac{\omega - i\left(\upsilon_i + \upsilon_e \frac{m_e}{m_i}\right)}{\omega}\right] \tag{46}$$

Substituting into equation (43) gives

$$k_\gamma = +\frac{\omega}{c}\left[1 + \frac{(\omega_p)_i^2}{\Omega_i^2}\left(1 - \frac{i\left(\upsilon_i + \upsilon_e \frac{m_e}{m_i}\right)}{\omega}\right)\right]^{(1/2)} \tag{47}$$

In our regime of interest

$$\frac{\upsilon_i}{\omega} << 1, \quad \frac{\upsilon_e \frac{m_e}{m_i}}{\omega} << 1$$

$$\frac{(\omega_p)_i^2}{\Omega_i^2} >> 1$$

Therefore

$$k_\gamma = \pm\frac{\omega}{c}\frac{(\omega_p)_i}{\Omega_i}\left[1-\frac{i\left(\upsilon_i+\upsilon_e\frac{m_e}{m_i}\right)}{\omega}\right]^{(1/2)}$$

$$\approx \pm\frac{\omega}{c}\frac{(\omega_p)_i}{\Omega_i}\mp\frac{i\left(\upsilon_i+\upsilon_e\frac{m_e}{m_i}\right)(\omega_p)_i}{2c\Omega_i} \quad = \quad \mathrm{Real}(k_\gamma)+i\,\mathrm{Imag}(k_\gamma) \tag{48}$$

$$\mathrm{Real}(k_\gamma) = \pm\frac{\omega}{c}\frac{(\omega_p)_i}{\Omega_i}$$

$$\mathrm{Imag}(k_\gamma) = \mp\frac{\left(\upsilon_i+\upsilon_e\frac{m_e}{m_i}\right)(\omega_p)_i}{2c\Omega_i} \tag{49}$$

This describes a wave having a phase velocity of $\approx \frac{c\,\Omega_i}{(\omega_p)_i}$ (which is the same size as the well known Alfven velocity) that is much slower than c. Since for the typical solar wind and IMF values,

$$\frac{\Omega_i}{(\omega_p)_i} = 5\times10^{-4} \text{ to } 2.5\times10^{-3}$$

The phase velocity $V_A \approx \frac{\omega}{k}$ ranges from 1.5×10^{-5} to 7.5×10^{5} meters/sec.

Since $E = B\,V_A$, a 2 nT disturbance has associated with it a 0.3 to 1.5 millivolt/meter electrostatic field.

Since the field varies as $e^{-[|\mathrm{Imag}(k)|]|r|}$, the distance over which the wave decreases to 1/e is given by

$$\xi = \frac{1}{\left|\text{Imag}\left(k_\gamma\right)\right|} = \frac{2c\Omega_i}{\left(\upsilon_i + \upsilon_e \frac{m_e}{m_i}\right)\left(\omega_p\right)_i} \qquad (50)$$

For typical solar wind values (n_i = 5/cc = 5(10^6) m/sec, B_{amb} = 2 nT, $(\omega_p)_i$ = 3(10^3)/sec, Ω_i = 0.5/sec, υ_e 2.5(10^6)/sec, υ_i = 2 (10^{-10})/sec, x = 6.9 (10^{13}) meter = 6.9 (10^{10})km. This implies that disturbances in the interplanetary region propagating in the direction of the ambient magnetic field (the solar sector structure magnetic field) are very weakly damped and essentially can propagate without significant retardation over distances large with respect to the scale size of the magnetosphere. In fact, there is little attenuation even over distances on the order of an a.u. (the distance between the earth and the sun). It is observed that several disturbances in the interplanetary region persist over distances up to a considerable fraction of an astronomical unit. Also, the solar sector structure clearly persists over several a.u. It is thus necessary to show that a portion of the interplanetary magnetic field is "born" with the solar wind and the field and plasma then move together away from the sun, each in a sense controlling the other.

We summarize this section on wave propagation in the direction of the ambient magnetic field by stating that such propagation can occur without significant attenuation and that such disturbances propagate approximately at the Alfven velocity.

2.3.3.3.2 Propagation Perpendicular to B

In the normal propagation mode

$$k_\gamma = 0$$
$$k^2 = k_T^2 = k_\alpha^2 + k_\beta^2$$

Setting $k_\gamma = 0$ in equation (35) and rearranging terms yields

$$\left[k_T^2 - \frac{\omega^2}{c^2}\left(1 + X_{\gamma\gamma}\right)\right]\left[k_T^2\left(1 + X_{\alpha\alpha}\right) - \frac{\omega^2}{c^2}\left(1 + 2X_{\alpha\alpha} + X_{\alpha\alpha}^2 + X_{\alpha\beta}^2\right)\right]\left[k_T^2 - \frac{\omega^2}{c^2}\right] = 0 \qquad (51)$$

The first factor $\left[k_T^2 - \frac{\omega^2}{c^2}(1+X_{\gamma\gamma})\right]$ has the same form as in the nonambient magnetic field configuration, and thus represents the same highly damped mode. This equation only involves Xgg and expanding the tensor in equation (17), it is seen that $X_{\gamma\gamma}$ affects only the E_γ term. Thus a wave propagating perpendicular to B_{amb} and having its E vector parallel to the ambient field is highly damped.

A similar expansion of the tensor in equation (17) shows that the term

$$\left[k_T^2(1+X_{\alpha\alpha}) - \frac{\omega^2}{c^2}\left(1+2X_{\alpha\alpha}+X_{\alpha\alpha}^2+X_{\alpha\beta}^2\right)\right] \tag{52}$$

represents a wave with both its propagation vector and its electric field vector oriented perpendicular to the direction of the ambient magnetic field.

To solve this mode we must solve

$$k_T^2(1+X_{\alpha\alpha}) - \frac{\omega^2}{c^2}\left(1+2X_{\alpha\alpha}+X_{\alpha\alpha}^2+X_{\alpha\beta}^2\right) = 0 \tag{53}$$

This gives

$$\begin{aligned} k_T &= \pm\frac{\omega}{c}\sqrt{\frac{1+2X_{\alpha\alpha}+X_{\alpha\alpha}^2+X_{\alpha\beta}^2}{1+X_{\alpha\alpha}}} \\ &= \pm\frac{\omega}{c}\sqrt{\frac{(1+X_{\alpha\alpha}+iX_{\alpha\beta})(1+X_{\alpha\alpha}-iX_{\alpha\beta})}{1+X_{\alpha\alpha}}} \end{aligned} \tag{54}$$

From equations (43) and (44) it is obvious that

$$\begin{aligned} 1+X_{\alpha\alpha}+iX_{\alpha\beta} &= 1+X_{\alpha\alpha}-iX_{\alpha\beta} \\ &\approx \left[1+\frac{(\omega_p)_i^2}{\Omega_i^2}\left(1-\frac{i\left(\upsilon_i+\upsilon_e\frac{m_e}{m_i}\right)}{\omega}\right)\right]^{(1/2)} \end{aligned} \tag{55}$$

Using the same magnitude approximations use in simplifying equation (45), one can show that

$$1+X\alpha\alpha = \frac{(\omega_p)_i^2}{\Omega_i^2} \tag{56}$$

$$k_T = \frac{\omega}{c}\frac{(1+X_{\alpha\alpha}+i\,X\alpha\beta)}{(1+X_{\alpha\alpha})^{(1/2)}}$$

$$= \frac{\omega}{c}\frac{(\omega_p)_i}{\Omega_i}\left[1 - \frac{i\left(\upsilon_i + \upsilon_e\frac{m_e}{m_i}\right)}{2\omega}\right] \tag{57}$$

This suggests that a wave propagating perpendicular to the background magnetic field will travel in the same mode as the case considered above for propagation parallel to the direction of the ambient magnetic field. Again, the wave will propagate with a velocity close to the Alfven speed.

2.4 Propagation of a disturbance in the IMF - Summary

Basically, in the above analysis we have represented the IMF as the superposition of electromagnetic waves. The only limitation of our investigation is that we must restrict it to wavelengths that are small with respect to the scale size of the magnetosphere. Thus we can examine only waves (or disturbances) with periods less than one hour. Although limited in this regard, our study sheds light on many aspects of the interaction of the IMF with the magnetosphere. These are briefly reviewed. We first summarize our findings on the propagation of electromagnetic disturbances in the solar wind.

The interplanetary field (represented as the superposition of several periodic electromagnetic waves) can persist only in the presence of the solar wind plasma. In the absence of a plasma, the presence of a time varying magnetic field in interplanetary space of the magnitude of only a few nT would have associated with it an electric field with a magnitude on the order of 1 volt per meter,

which is at least three orders of magnitude larger than the magnitude of electric fields observed in the interplanetary region.

In the solar wind, in the absence of a background ambient magnetic field, any disturbances with periods on the order of minutes to hours will be rapidly attenuated unless they are driven continuously in a local region. Electromagnetic disturbances in the solar wind can persist only in the presence of an ambient (lower frequency) magnetic field. When such conditions are present (the presence of both plasma and "background" magnetic field) electromagnetic waves with periods from a few minutes to several hours can propagate over distances large with respect to the distance from the Sun to the Earth without appreciable attenuation. The background (ambient) magnetic field is provided by the "solar sector magnetic field" which is co-produced with the solar wind. It moves outward from the sun with the solar wind, and has a period of about two weeks - much longer than the characteristic periods of the electromagnetic disturbances being considered. Electromagnetic waves allowed in the interplanetary medium propagate at the Alfven speed. There are two wave modes that propagate without appreciable attenuation.

1. When the propagation vector is parallel to the ambient magnetic field.

2. When both the propagation vector and the disturbance electric field are perpendicular to the ambient magnetic field direction.

Each of these cases is represented schematically in Figure 3. It then was a simple exercise to examine the interaction of such waves when they encountered a discontinuity in plasma (the magnetopause).

2.5 Interaction of a Disturbance With the Magnetosphere

In the previous sections we have described the propagation of an electromagnetic wave in a tenuous magnetized plasma. When this wave interacts with the magnetosphere at the magnetopause, we must investigate the waves interaction with a discontinuity in the plasma or in the ambient magnetic field. We must understand how electromagnetic wave interact with discontinuities, and how the waves reflect and refract in the presence these discontinuity.

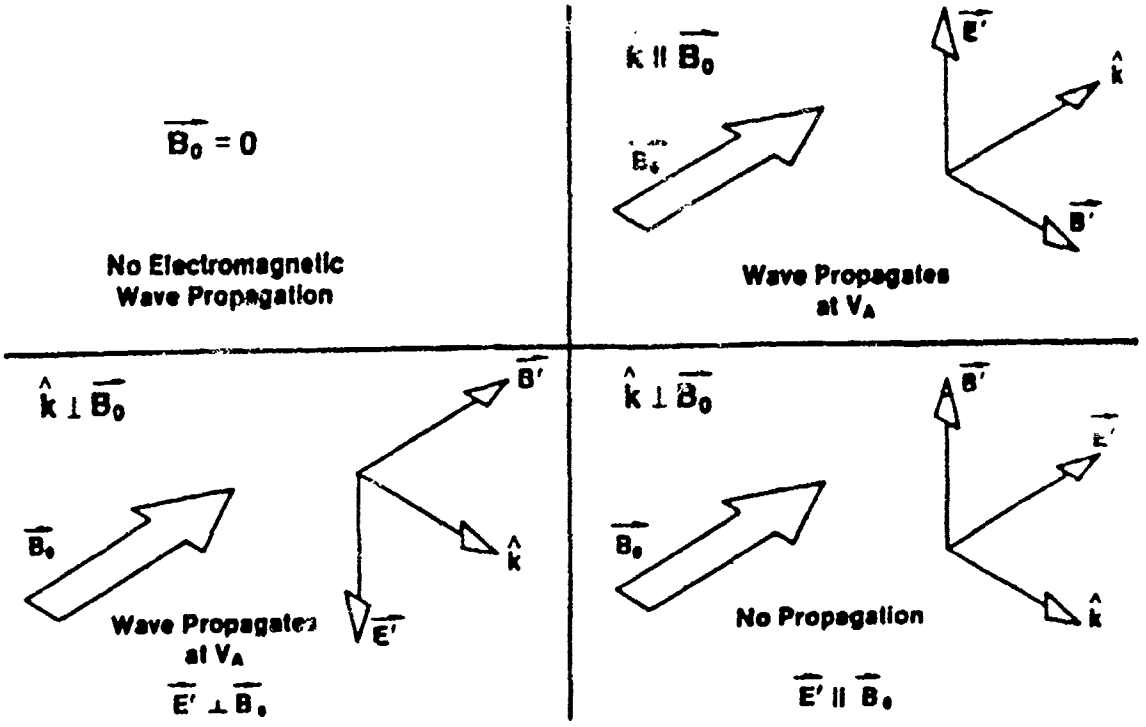

Figure 3. Electromagnetic wave propagation in a tenuous plasma. The wave propagates with little attenuation when its propagation vector is parallel to the direction of the ambient magnetic field, and when the propagation vector and the disturbance E vector are perpendicular to B.

At the magnetopause, the propagation of the electromagnetic disturbances will been in accordance with Snell's law (note: Snell's law is valid even for anisotropic media). Thus

$$k_{in} \sin(qin) = k_{out} \sin(\theta_{out})$$

where k_{in} and k_{out} are the propagation vectors inside and outside the magnetopause and θ_{in} and θ_{out} are the angles the k vector makes with the normal to the interface surface. Snell's law holds for a plane wave interacting with an infinite flat surface. This is a good approximation over the tail fo the magnetopause. In the nose and dayside cusp regions of the magnetopause region, it can be used only as a semi-quantitative indicator.

If $k_{out}/k_{in} <= 1$ (i.e., the same order or smaller), then the disturbance can enter

through the interface for all angles of incidence. If, however, k_{out}/k_{in} is large, then entry can occur only for perpendicular incidence ($\theta_{out} = 0$).

In the previous sections we have shown that for low frequency disturbances of interest, only Alfven-like modes can propagate and then only in the presence of a d.c. magnetic (i.e., the disturbance must be superimposed on a steady state field). Using the definitions of the plasma frequency, ω_p, and the cyclotron frequency, Ω_i, we can write

$$\frac{k_{out}}{k_{in}} = \frac{\left[(\omega_p)_i\right]_{out}}{\left[(\omega_p)_i\right]_{in}} \cdot \frac{(\Omega_i)_{in}}{(\Omega_i)_{out}}$$
$$= \left(\frac{n_{out}}{n_{in}}\right)^{1/2} \cdot \frac{(B_{amo})_{in}}{(B_{in})_{out}} \qquad (58)$$

We can now estimate the ratio k_{out}/k_{in} when $n_{out} = 5/cm^3$ and $(B_{amb})_{out} = 2$ nT. For various magnetospheric conditions

N_{inside}	B_{inside}	k_{out}/k_{in}	Entry
$1.0/cm^3$	50nT	55	poor
$10./cm^3$	2nT	.4	good
$01/cm^3$	2nT	1.4	Okay
$0.1/cm^3$	2nT	4.4	Marginal

Thus entry into a magnetospheric region of high field strength or into a very rarefied plasma region is difficult, whereas entry into a denser plasma region or into a weak field region is relatively easy. For example, the wave can penetrate the flanks of the tail with relative ease (i.e, all directions of the k vector can enter), whereas entry near the tail lobes is difficult.

Since we expect transmission of the wave through various portions of the boundary, especially the flanks of the tail, an estimate of the transmission factors must

be made. The actual matching of the fields at the boundary of an anisotropic medium is quite complicated. However, for normal incidence the problem is quite straight forward since the Fresnel ratios are the same as for isotropic media. Thus

$$\frac{E_{in}}{E_{out}} = \frac{2\,k_{out}}{k_{out}+k_{in}} = \frac{2}{1+\frac{k_{in}}{k_{out}}}$$

$$\text{if } \frac{k_{out}}{k_{in}} = 5 \text{ then} \qquad (59)$$

$$\frac{E_{in}}{E_{out}} = 0.67$$

The associated magnetic field are

$$\frac{B_{in}}{B_{out}} = \frac{k_{in}}{k_{out}} \cdot \frac{E_{in}}{E_{out}} \approx 2\,(.67) \approx 1.3 \qquad (60)$$

For an interplanetary magnetic disturbance incident perpendicular to the magnetopause, reflection and transmission can be calculated. In this example, the magnetic field disturbance has a larger B amplitude within the magnetosphere than in interplanetary space.

For the wave to propagate inside the magnetosphere, the E vector of the disturbance must be perpendicular to the magnetospheric magnetic field and thus the B disturbance vector must be parallel to magnetospheric magnetic field. If the B disturbance vector is perpendicular to the magnetospheric field, it will be damped out. For a perpendicular incident wave, the ambient solar field must be in the y direction. When the solar field is in the y direction (Note: x is toward the sun, y is toward dusk and z points north), the disturbance field outside can have its B vector parallel to the magnetospheric field. If the ambient B outside were in the x direction and the wave propagating perpendicular to the boundary (k vector in the y direction), then the B disturbance vector must be parallel to the external ambient (in the x direction) and thus on passing through the boundary would be perpendicular to the internal ambient and be damped out after entry. Figure 4 shows an example of a disturbance passing through the magnetopause and propagating within the magnetopause.

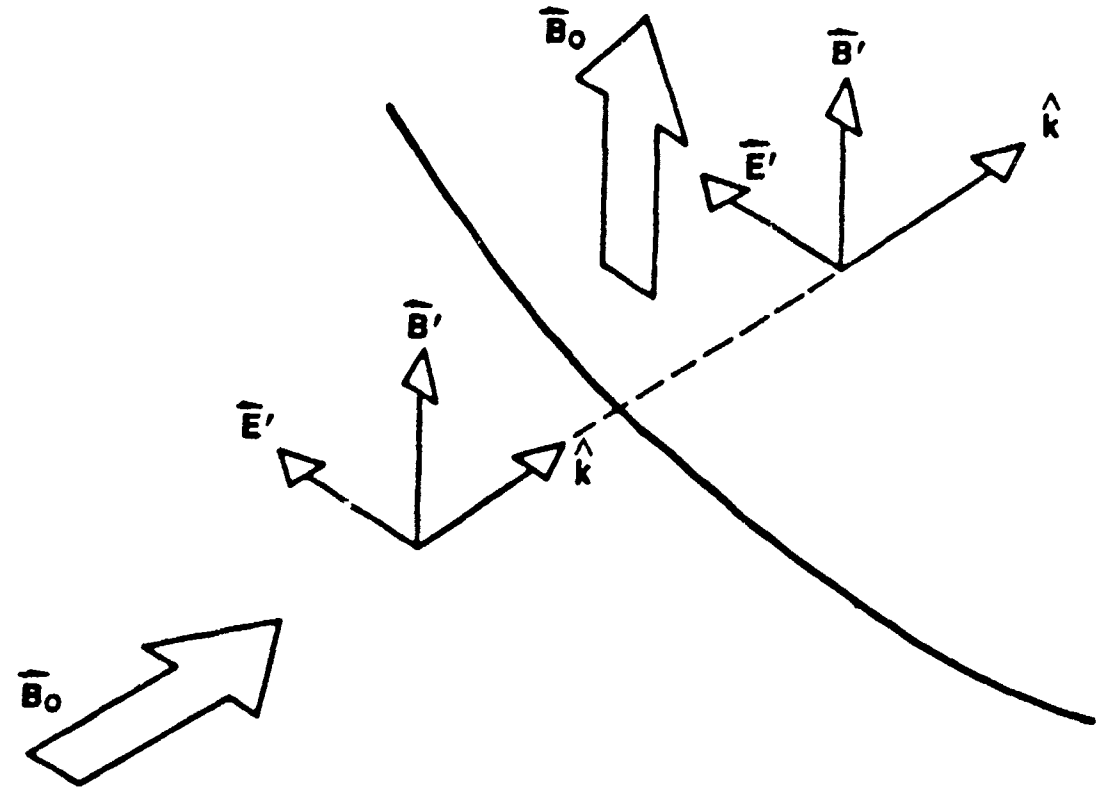

Figure 4. Transmission through the magnetopause and propagation in the magnetosphere. This process is completely analogous to the passage of light from vacuum into glass. In both media (the interplanetary region and in the magnetosphere) the disturbance $\underline{E}$ vector must be perpendicular to the ambient magnetic field direction.

2.6 Effects of the IMF Disturbances within the Magnetosphere

The basic problem of magnetospheric physics remains the explanation of the response of the magnetosphere to variations in the solar wind and the IMF. So far we have shown that we can represent disturbances as waves and that these waves after interacting with the magnetopause can in certain locations and with certain preferred directions enter the magnetosphere.energization processes in the magnetotail. The solar wind is represented as a tenuous plasma with an imbedded magnetic field, the well known solar sector structure magnetic field. Higher frequency waves can propagate in this medium with the Alfven speed if their propagation direction is parallel to the sector structure magnetic field. Such waves can also propagate if the propagation vector is perpendicular to the sector

structure magnetic field providing the wave's electric field. The study also determined that when the wave interacts with the magnetopause, the wave is either reflected or transmitted. The study determined that transmission was possible only near the equatorial flanks of the tail and near the cusp regions, regions of weak magnetic field and where the plasma density inside the magnetopause was relatively high. Once the wave has penetrated through the boundary of the magnetosphere, it will either travel at the local Alfven speed or be absorbed. It was determined that only waves whose magnetic field vector oscillates in the north/south direction are capable of propagating in the interplanetary medium, pass through the boundary near the equatorial flanks and then propagate within the magnetospheric tail field region.

Variations in the north south component of the interplanetary field have long been associated with substorm triggers. To begin the study of substorm trigger, studies of the magnetic field variations in the magnetospheric tail in response to changes in the IMF were initiated. The effort has focused on the development of a model of the magnetospheric tail that included an arbitrary north south wave propagating through the tail at the Alfven speed and the evaluation of the extent to which this traveling wave can act as a substorm trigger. A newly revised dynamic magnetic field model was used as the starting point of the study. The new dynamic magnetic field model consists of four separate magnetic field routines, an internal field routine, a magnetopause magnetic field routine, a ring current magnetic field routine, and a tail current magnetic field routine. The model developed for the IMF wave entering the magnetopause and then propagating within the magnetosphere was written as a time dependent routine which was then combined with the other four existing routine to produces a time dependent magnetic field model.

We have shown that a disturbance pulse can enter the magnetosphere. Once the disturbance pulse is within the magnetosphere it propagates down and across the tail at the Alfven speed. We now discuss the development of a dynamic model of the magnetosphere that included a propagating wave within the magnetosphere. The effort used the equations developed earlier to create a computer model for the magnetospheric tail that includes the effects of a variation in the IMF.

The computer model of the disturbance pulse begins with a disturbance pulse in the IMF. The disturbance pulse model that has been developed includes the following options:

1. The IMF disturbance can either be north or south (small dawn dusk variations were also modeled).

2. The rise time of the disturbance vector is adjustable. The shape of the rising edge of the disturbance vector was assumed to have a sinusoidal shape (quarter period) of arbitrary duration.

3. The duration of the pulse is adjustable. If the pulse has a finite length, the fall time of the pulse is adjustable. The falling portion of the pulse is also a quarter of a sinusoid.

A specified disturbance having a profile determined by the above constraints is initiated outside the magnetosphere and then allowed to interact with the magnetopause. The wave which enters the magnetosphere near the equator and along the flanks is then allowed to modify the magnetospheric magnetic field.

Five distinct disturbances were modeled, they are:

1. A 4 nanotesla northward disturbance with a rise time of 5 R_e and an infinite pulse length.

2. A 4 nanotesla northward disturbance with a rise time of 5 R_e and a fall time of 5 R_e.

3. A 4 nanotesla southward disturbance with a rise time of 5 R_e and an infinite pulse length.

4. A 4 nanotesla southward disturbance with a rise time of 5 R_e and a fall time of 5 R_e.

5. A 4 nanotesla shouthward disturbance with a rise time of 5 R_e and a fall time of 5 R_e having a 1.0 nanotesla dawn dusk variation. Two cases were examined, the first considers propagation in the anti-solar direction, the second propagation along the garden hose angle.

Figure 5 shows the space profile of the north south variation in the IMF. Since the pulse is traveling through the IMF with the Alfven speed, the pulse has definite spatial extent. When the leading edge of the pulse is at a given location, the pulse maximum is some distance upstream. For presentation purposes it is easiest to display the figures as a function of location with each figure describing the magnetic field topology at a fixed time. The pulses used for these test cases were assumed to have their propagation vectors in the ecliptic plane and make a 45 degree angle (approximately along the garden hose angle) with the sun-earth line. The effect of these disturbance pulses on the magnetospheric magnetic field is shown by displaying the behavior of the magnetic lines of force in the noon-midnight meridian plane.

2.6.1 Northward Pointing Disturbance

Figure 6 shows the magnetic lines of force within the magnetospheric tail in the noon-midnight meridian plane. The field lines are spaced one degree apart in the high latitude intercept of the earth. They vary in latitude from 60 degrees to 75 degrees. The top panel is the quiet time magnetic field with only the magnetopause, ring and tail currents contributing to the magnetic field. A northward pointing disturbance of 4 nanotesla having a rise time of 5 R_e and long persistence is allowed to interact with the magnetosphere. The second panel shows the magnetic field topology when the leading edge of the disturbance pulse has reached the -20 R_e. The remaining panels show the changes in the magnetic field topology as the pulse propagates down the tail. The northward disturbance strengthens the z-component of the magnetic field in the tail and thus produces a more dipolar tail field geometry. When a short northward disturbance is allowed to propagate down the tail, the results are very similar to the above result with the long pulse. The field becomes more dipolar in a limited region of space. Once the pulse has passed, the field recovers to its initial configuration.

The increasing tail strength due to the entering disturbance wave has many interesting implications. The long pulse reduces the magnetic field gradients along the flanks of the tail and thus reduces the amount of magnetosheath plasma that can enter across the magnetospheric boundary. The enhanced field within the tail increases the magnetic current limit, and thus increases the allowed plasma sheet current densities. Thus the electric field strength in the boundary layer as well as the cross tail electric field must change in response to

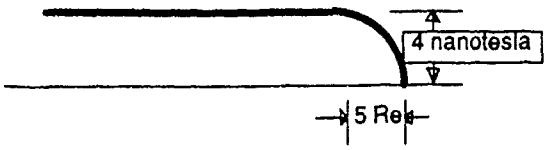

4 nanotesla northward pulse rising to peak value over a distance of 5 R_e

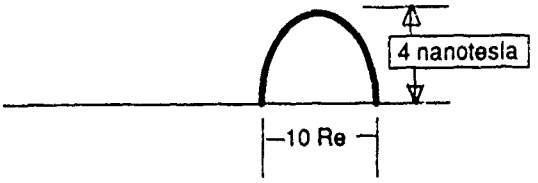

4 nanotesla northward pulse rising to its peak value in a distance of 5 R_e and then decaying again to zero

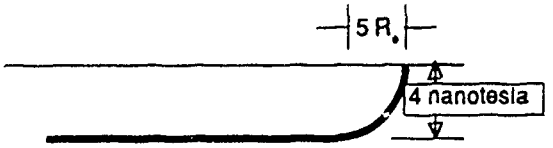

4 nanotesla southward pulse rising to peak value over a distance of 5 R_e

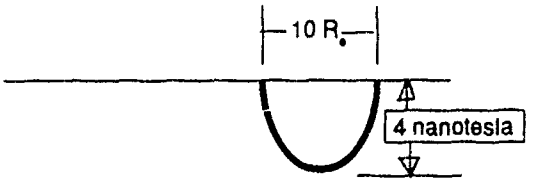

4 nanotesla northward pulse rising to its peak value in a distance of 5 R_e and then decaying again to zero

Figure 5. The above four schematics show the disturbance pulses. The tail magnetic field model was subjected to the four types of disturbances shown above. The pulse moves from left to right at the Alfven speed.

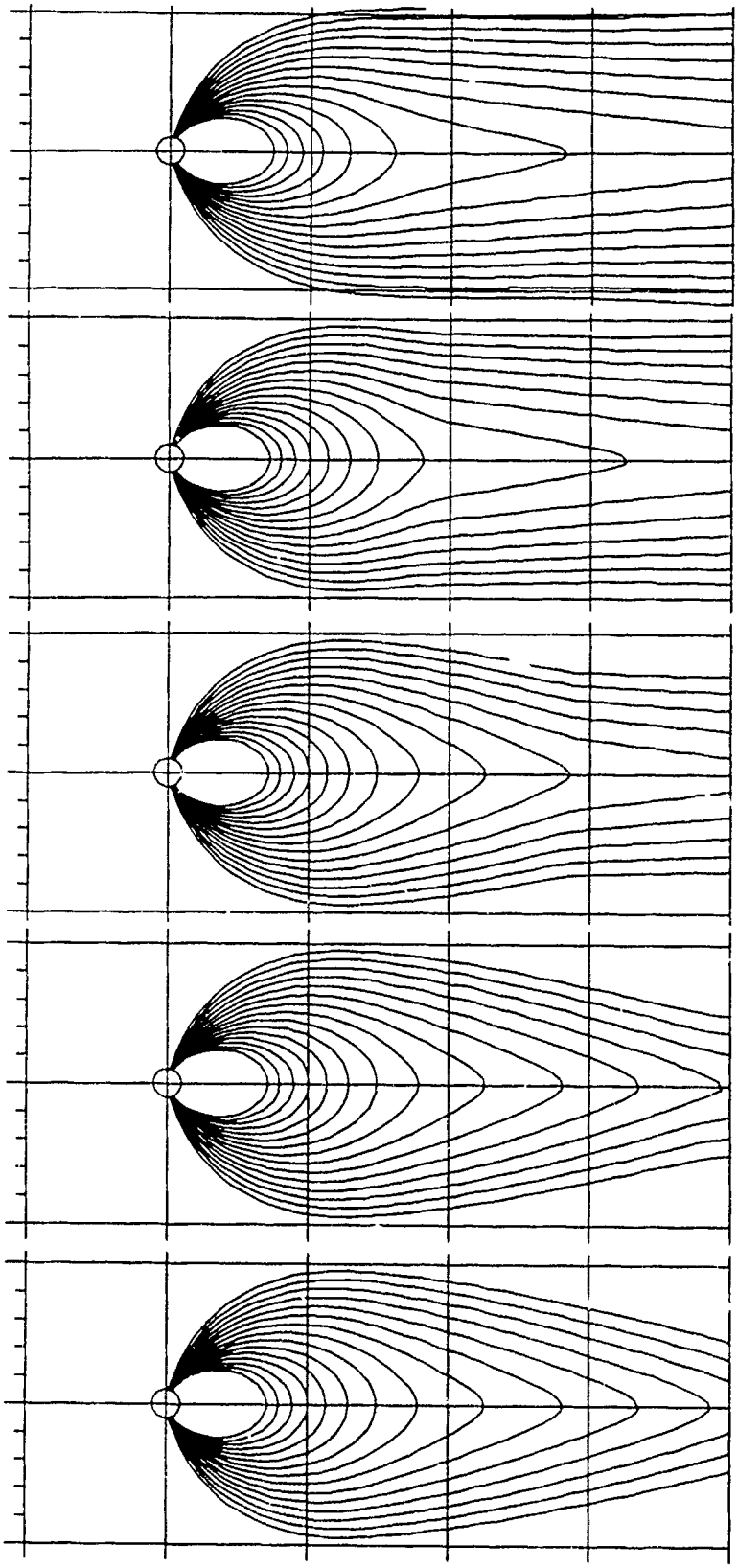

Quiet time - field lines using Magnetopause, Ring and Tail current systems only

Leading edge of disturbance is at -20 R_e

Leading edge of disturbance is at -30 R_e

Leading edge of disturbance is at -40 R_e

Leading edge of disturbance is at -50 R_e. Note: Dipole-like compressed tail.

Figure 6. Noon midnight meridian cross section of the tail showing the propagation of a northward pointing disturbance. Pulse is a long 4 nanotesla northward pulse.

these variations in the magnetic field and magnetic field gradients. The effect of these changes on the plasma and on the electric fields have not yet been determined.

2.6.2 Southward Pointing Disturbance

Figure 7 shows the magnetic field lines in the noon-night meridian plane when a southward disturbance propagates through the magnetosphere. The disturbance pulse rises over a distance of 5 R_e and remains at the disturbance level for an extended time (see figure 5). The top panel represents the quiet magnetosphere before the arrival of the pulse. The next panel shows the tail field topology when the leading edge of the pulse is at -20 R_e. Subsequent panels show the leading edge moving in the anti-solar direction. It can be seen that the pulse results in a weakening of the tail and that the tail takes on a more taillike appearance (i.e. the tail becomes extended). When the pulse is at distances larger than -30 R_e, the figures show a bulge in the field lines near the neutral sheet (i.e. the field lines no longer appear to cross the neutral sheet). To investigate the behavior of the field lines in this case it is necessary to generate a second set of field line plots, a set where all field lines are forced to originate from the equator. Figure 8 shows the same case but in this figure the displayed field lines originate at the equator instead of the polar cap. One can see that pulse creates an "O" and an "X" type neutral point. There is a set of field lines that is no longer connected to the polar cap and this set of field lines moves in the anti-solar direction along with the disturbance pulse. For this long extended pulse the "O" type neutral point moves down the tail, whereas the "X" type neutral point remains fixed near -20 R_e.

Figure 9 is similar to Figure 8 except that the disturbance pulse is short. The pulse rises from 0 to 4 nanotesla in 5 R_e and then decays to zero over a distance of 5 R_e. Once again the top panel is the undisturbed configuration and subsequent panels show the disturbance pulse at different locations in the tail. In this figure both the "X" and "O" type neutral point move down the tail at the speed of the disturbance.

The behavior of the field lines when a southward disturbance is introduced is similar to the "plasmoid" topology often described by experimentalist. The southward disturbance significantly weakens the field in the tail neutral sheet. It actu-

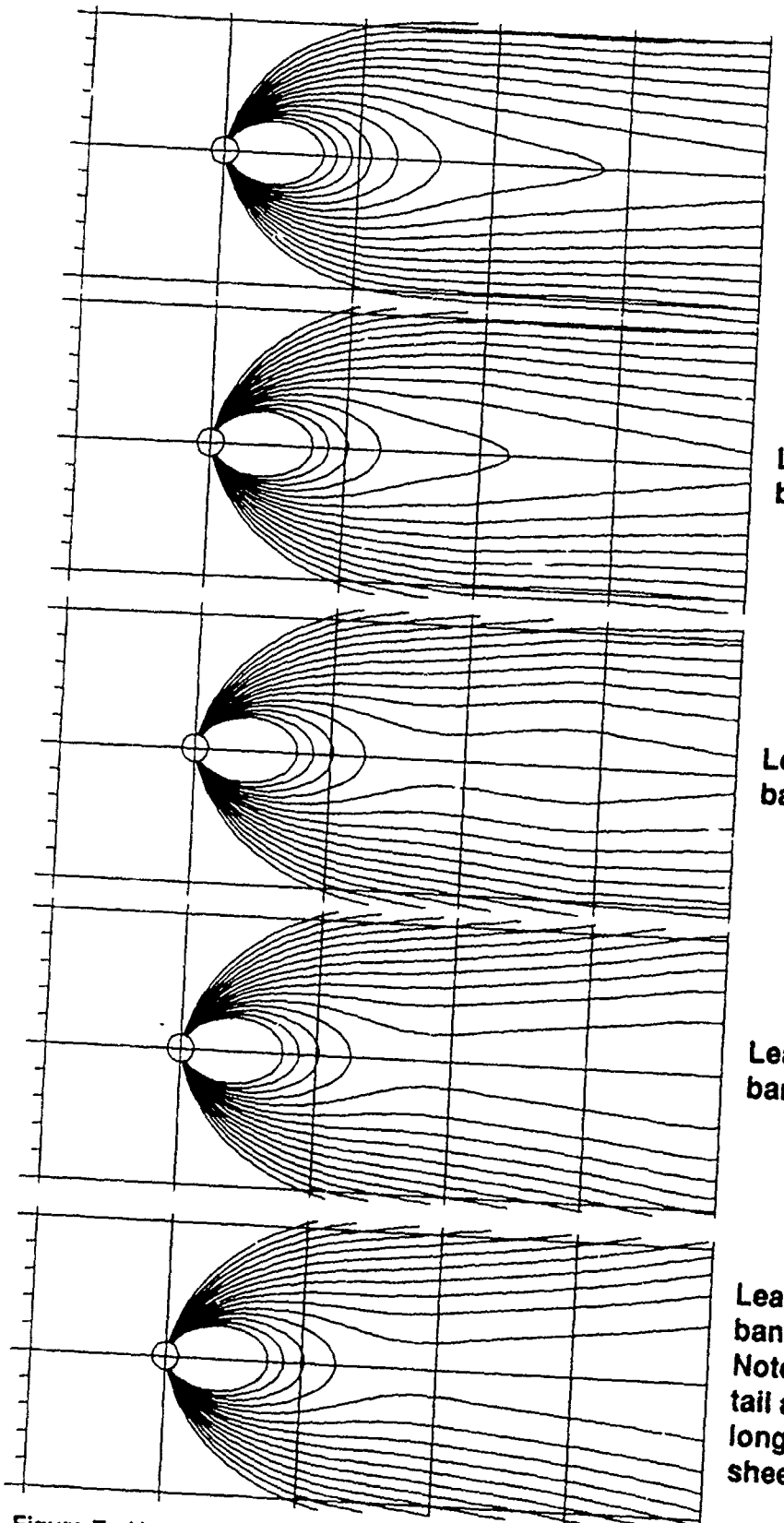

Figure 7. Noon midnight meridian cross section of the tail showing the propagation of a southward pointing disturbance. Pulse is a long 4 nanotesla southward pulse.

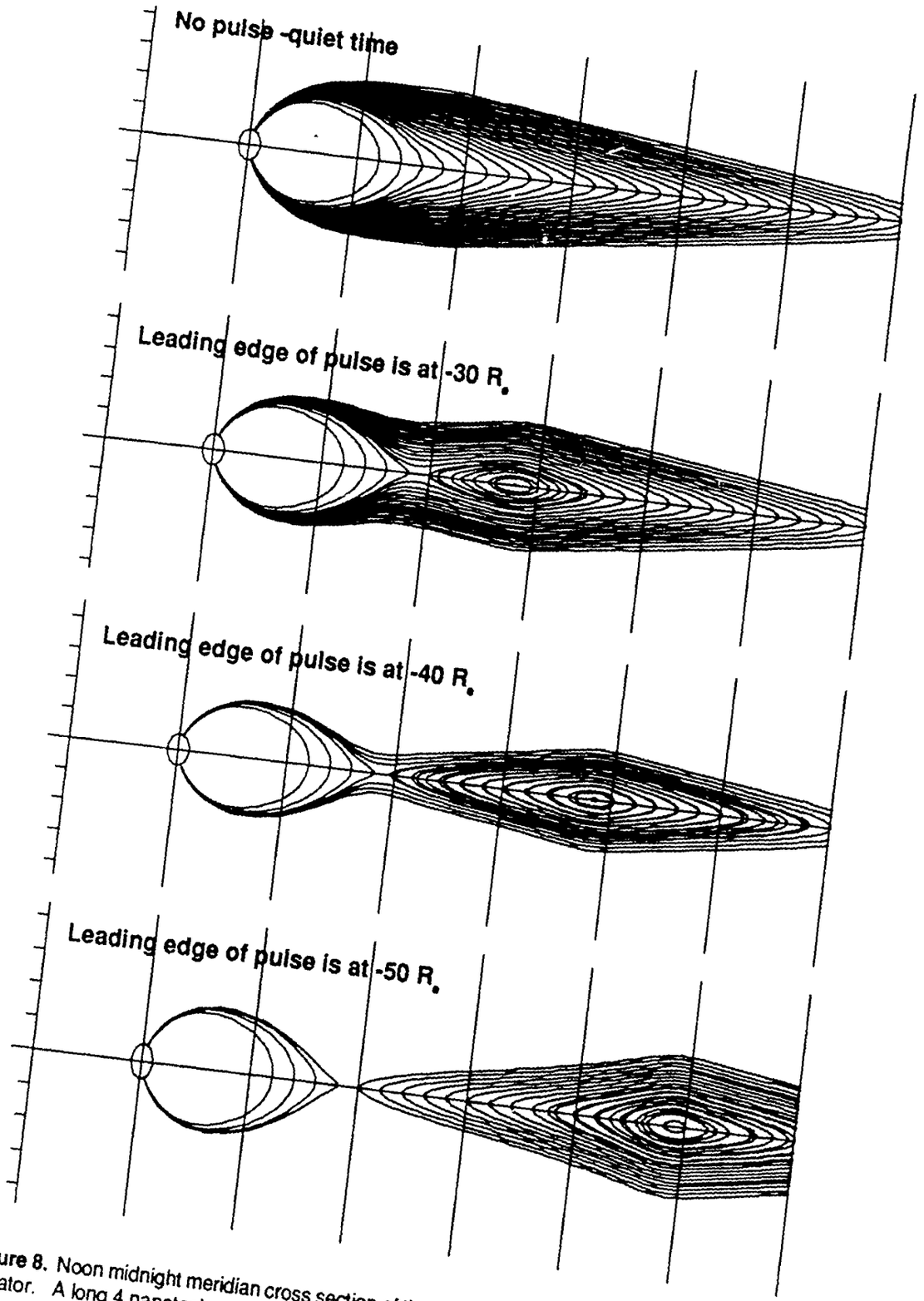

Figure 8. Noon midnight meridian cross section of the magnetosphere. Field lines are drawn from the equator. A long 4 nanotesla pulse moves down the tail. Note the 'X' and 'O' type neutral points.

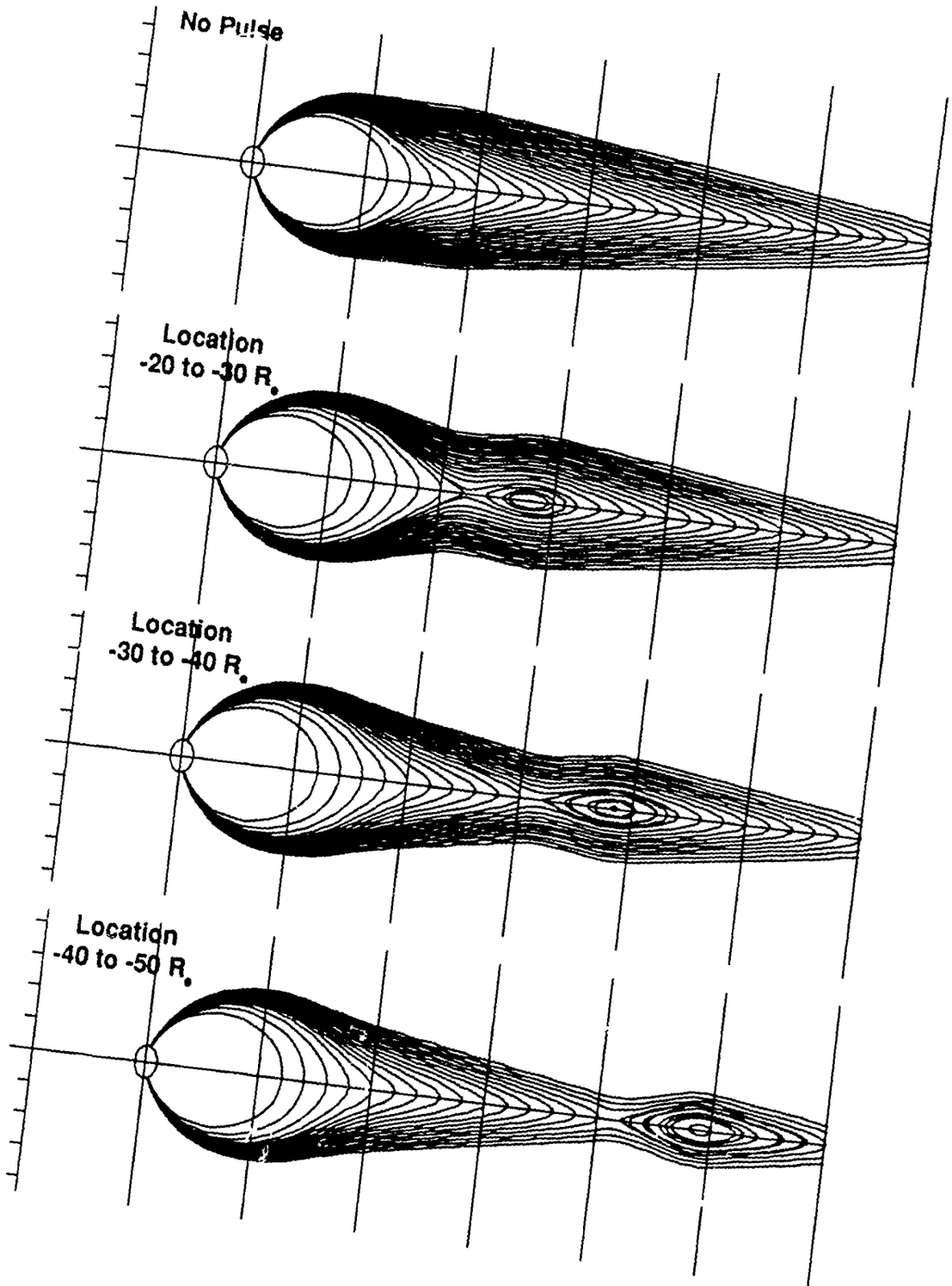

Figure 9. Noon midnight meridian cross section of the magnetosphere. Field lines are drawn from the equator. A short 4 nanotesla pulse moves down the tail. Note the 'X' and 'O' type neutral points. The disturbance pulse rises in a distance of 5 R_e and than decays back to zero in a distance of 5 R_e.

ally reverses the field over a region of the neutral sheet and thus produces the neutral points. The weakening of the field reduces the amount of plasma the field can support and the magnetically limited currents are drastically reduced. This analysis is a first step and includes only the first order effects of the propagating magnetic wave. It does not as yet include the effects of the plasma response. The plasma response is expected to significantly alter the behavior of the pulse because the beta of the plasma near the neutral point will exceed one unless the plasma rearranges itself in response to the magnetic field.

2.6.3 Southward Pointing Disturbance Accompanied by a Dawn Dusk Variation.

A wave travelling in the IMF along the garden hose field line can have variations in the ecliptic plane as well as variations perpendicular to it. The previous examples consisted only of waves having magnetic variations perpendicular to the ecliptic plane. We now consider a wave that has the same variation perpendicular to the ecliptic plane and also has a magnetic variation in the ecliptic plane. This wave has the same propagation properties in the IMF as the previous waves and the interaction at the magnetopause is the same. However, when this wave enters into the magnetosphere parts of the wave are damped. The dawn dusk component of the wave has an electric field vector perpendicular to the equatorial plane and thus the dawn dusk component is damped in the center of the plasma sheet. Near the edges of the plasma sheet, the dawn dusk variation can, however, propagate through the tail. Figure 10 is a 3-dimensionally picture of a field line in the plasma sheet when the disturbance containing both north south and dawn dusk variations is propagating in the anti-solar direction. The superposition of the field from the IMF with the magnetic field of the magnetosphere gives rise to a spiral field line topology. Such spiral field line topologies have been postulated by experimentalists and are often referred to as 'flux ropes'.

Figure 11 shows a field line in the plasma sheet when the north south and dawn dusk disturbance propagates across the tail at a 45 degree angle. The wave enters on the dusk side and propagates down the tail and moves from dusk to dawn. The spiral field line topology has developed in only a portion of the plasma sheet. The ends of this spiral connect to either the ionosphere or the distant tail. The example in Figure 11 shows a connection to the ionosphere.

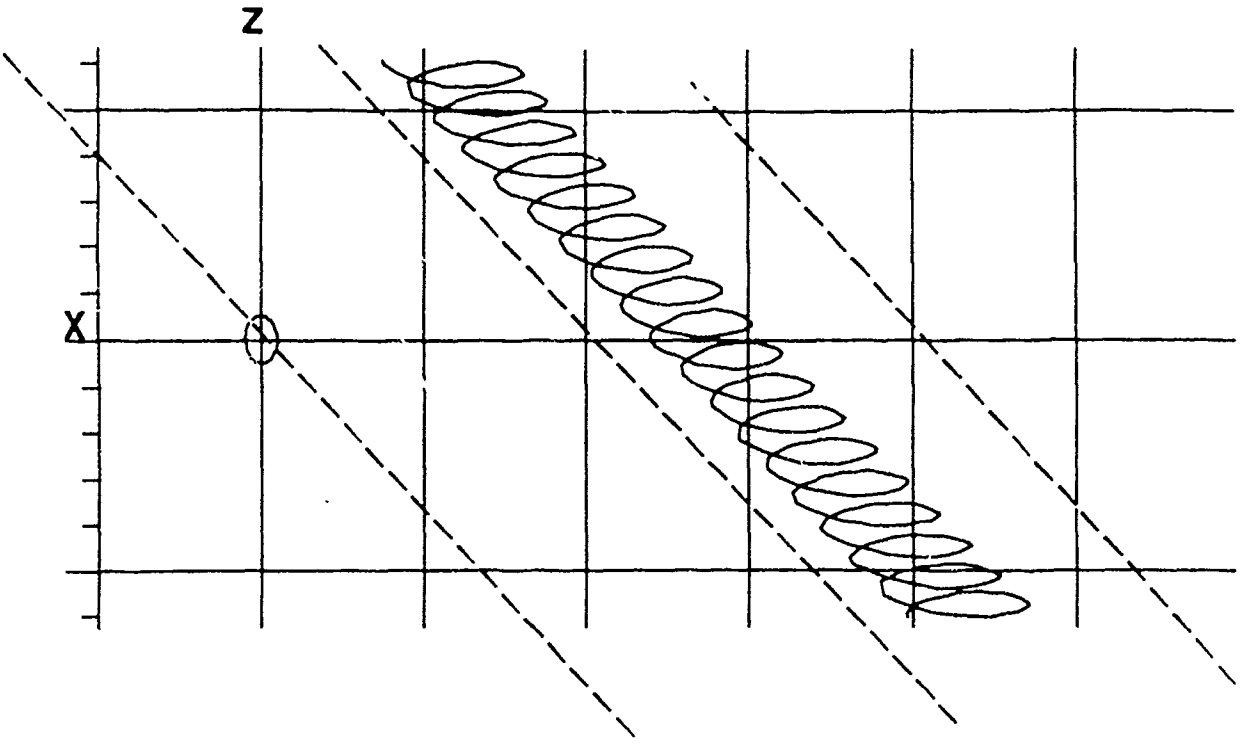

Figure 10. A 4 nanotesla southward IMF pulse with a 1 nanotesla dawn dusk component. Pulse is travelling in the anti-solar direction. The 'Flux Rope' lies in the equatorial plane extending

The examples in Figures 10 and 11 demonstrate the simplicity of creating very complex structures within the magnetotail, structures that have been experimentally observed on numerous occasions. Many complex theories have been created to explain the existence of these structures. This study, however, suggests that a simple interaction between the magnetic variations in the IMF and the magnetospheric magnetic fields can also be used to explain the observations.

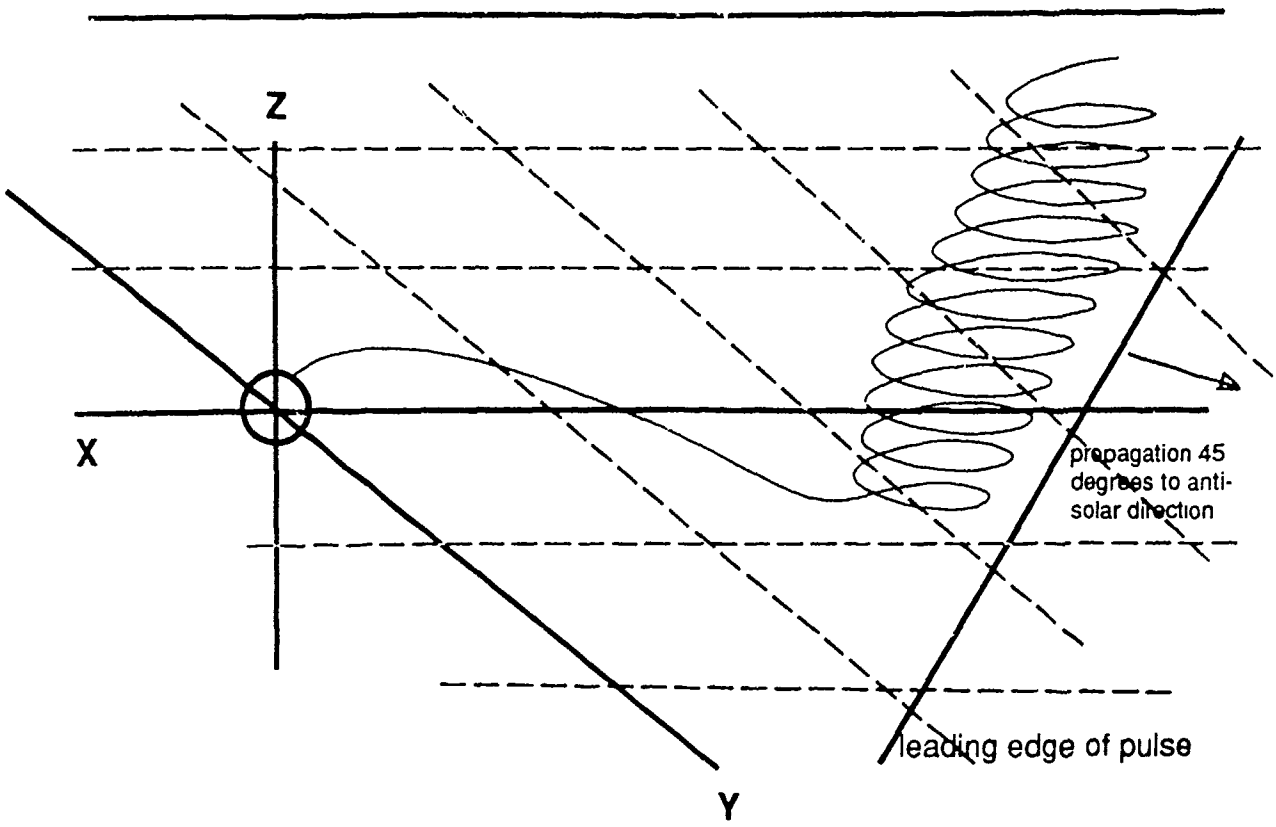

Figure 11. A 4 nanotesla southward pulse with a 1 nanotesla dawn dusk component propagating through the plasma sheet. The propagation direction is 45 degrees to the x-axis. The 'Flux Rope' lies in equatonal plane and extends part way across the tail with the field line terminating in the ionosphere

3.0

SUMMARY

The models of the disturbance wave propagating within the tail of the magnetosphere are the first of a series of steps necessary to develop a comprehensive understanding of magnetotail dynamics. This work in conjunction with the work on particle entry into the magnetosphere provides a detailed understanding of magnetospheric particle energization. The magnetic field model of the disturbance magnetic field when combined with the existing dynamic magnetic field model provides a tool for evaluating the response of the plasma to the magnetic stimulus of the IMF. This effort will ultimately permit us to understand the role of the IMF in controlling and/or triggering processes within the magnetosphere.

The equation on wave propagation and wave penetration into the magnetosphere are based on Maxwell's equation. They present a novel new method for studying the interaction magnetic variations in the solar wind with the plasma inside the magnetosphere.

The dynamic model of the plasma sheet magnetic field developed as a part of this effort includes variations in the IMF and can be used to study the response of the tail to external stimuli. Although much work has been done, much additional work needs to be done. The above described model is not completely self consistent. Although solutions to Maxwells equations were used in arriving at the propagation equations, the response of the local plasma to this traveling wave is not treated self consistently. During large distrubances the beta of the plasma in the plasma sheetcan be very close to unity. Thus when a southward disturbance weakens and at time even reverses the field in the plasma sheet the organizing ambient magnetic field disappears, and the cross tail currents are explosively disrupted with a release of a considerable amount of energy. It is apparent from this study that the changes in the plasma sheet produced by the interaction of the IMF with the magnetospheric magnetic field produce changes that are more than adequate to produce the variations observed during a sub-storm. A complete quantitative model of a sub-storm must include not only these triggering effects but also the response of the plasma sheet plasma to this variation.

The model of the plasma sheet developed under this effort is relatively simple, but provides considerable insight into some of the observed variations within the plasma sheet. Many of the complex magnetic field topologies that have been postulated by various experimentalists to explain complex magnetic field and charged particle observations can be reproduced by this analysis.

Considerable progress has been made in understanding the dynamics of the magnetotail. We have developed a dynamic model of the magnetotail magnetospheric magnetic field. We have furthermore attempted to find a unique set of satellite observations that would unambiguously verify our proposed theory. This effort has not been completely successful. We can reproduce magnetic field and charged particle topologies, but a theory must be used to predict in order to be completely validated. We must use charged particle and magnetic field measurements in the solar wind to predict the onset and intensity of substorms. This requires the use extensive correlative measurement in the solar wind and in the tail regions of the magnetosphere. The CDAW workshops have extensive correlative data within the magnetsophere for very isolated events but lack many of the solar wind measurement required to do the prediction. We must have sufficiently accurate data of the B and E fields in the solar wind so that the propagation vector, k, can be determined. Once the k vector is determined for many events, correlation with substorm onsets and intensity can be performed and a comparison can be made with this theory. This requires the use of vast amounts of data both inside and outside of the magnetosphere. Such use of large amounts of data was beyond the scope of this effort and must be delayed for a future effort.